A NIR fluorescent probe for Fatty Acid Amide Hydrolase bioimaging and its application in development of inhibitors

Manman Tian [a +], Zhenhao Tian [c +], Dahong Yao [d +], Jing Ning [a], Sa Deng [a], Lei Feng [a,e *], Xiaokui Huo [a], Xiangge Tian [a *], Baojing Zhang [a], Chao Wang [a], Zhenlong Yu [a], Xiaochi Ma [a,b *]

[a] The Second Affiliated Hospital, College of Pharmacy, Dalian Medical University, Dalian, China;

[b] Jiangsu Key Laboratory of New Drug Research and Clinical Pharmacy, Xuzhou Medical University, Xuzhou, Jiangsu 221004, China;

[c] School of Life Sciences, Northwestern Polytechnical University, Xi'an, 710072, China.

[d] School of Pharmaceutical Sciences, Shenzhen Technology University, Shenzhen, 518118, China;

[e] School of Chemistry and Chemical Engineering, Henan Normal University, Xinxiang 453007, China.

* Corresponding authors: maxc1978@163.com, tianxiangge1990@163.com and leifeng@dmu.edu.cn

[+] Theses authors contribute equally.

1. Materials and methods

1.1 Material and instruments

The fatty acid amide hydrolase used in this study was recombinant enzyme from 293T [1]. BV2, U251 and C6 cells were purchased from American Type Culture Collection. Cell culture medium (DMEM) and fetal bovine serum (FBS) are purchased from Gibco-BRL Co. Hoechst33342, lipopolysaccharide (LPS), HSA (Human serum albumin), *β*-Glu (*β*-Glucuronidase), AchE (acetylcholinesterase) and PGA (Penicillin G acylase) were obtained from Sigma Aldrich; URB597 is purchased from Selleck chemical. BCA protein quantitative kit is purchased from Elabscience. CES1B (Carboxylesterase 1B), CES2 (Carboxylesterase 2), CYP3A4 (Cytochrome P450 3A4) and Lipase were purchased from Corning Gentest. iNOS, COX2 and Actin primary antibody were purchased from Cell Signaling Technology as well as all secondary antibodies. All other solvents and reagents involved in this study are the highest-grade reagents on the market. All fluorescence analysis was conducted on Synergy H1 microplate reader (Bio-Tek). All chromatographic analyses were performed by Water e2695 HPLC.

1.2 Synthesis Pathway for DAND.

Synthesis of **DAN**: Compound **DDAN** was prepared according to previous report[2]. To a solution of **DDAN** (612.1 mg, 2.0 mmol) in ethanol (50 mL) under an argon atmosphere was added 80% hydrazine hydrate (2 mL) and 10% Pd/C (64.3 mg, 0.06 mmol), then the mixture was refluxed for 3 h. When the TLC confirmed no starting material remained, the mixture was filtered and the filtrate was concentrated under reduced pressure. The residue was then dissolved in ethyl acetate (50 mL), and the aqueous solution of $NaIO_4$ (30 mL, 0.1 M) was added, the reaction mixture was vigorous stirred for 30 min. Then, the phases were separated and the organic layer was washed with brine, dried over anhydrous Na_2SO_4, filtered, and concentrated. The residue was further purified by a silica gel column chromatograph using CH_2Cl_2/MeOH (40/1, *v/v*) as the mobile phase to afford **DAN** as a violet solid (403.3 mg, yield 84.7%). HRMS (ESI positive) calced for $[M+H]^+$ 239.1179, found 239.1178 (**Scheme S1, Fig. S1-S2**).

Synthesis of **DAND**. To a solution of decanoic acid (103.3 mg, 0.6 mmol) in 5 mL anhydrous N, N'-dimethylformamide (DMF) at 0 °C under an argon atmosphere, 2-(7-azabenzotriazol-1-yl)-N, N, N', N'-tetramethyluronium hexafluorophosphate (HATU, 228.1 mg, 0.6 mmol) and N, N-diisopropylethylamine (DIEA, 77.5 mg, 0.6 mmol) were added sequentially, the reaction mixture was stirred for 1 h. Then, a solution of **DAN** (71.4 mg, 0.3 mmol) in 3 mL anhydrous DMF was slowly introduced, and the reaction mixture was stirred at room temperature for 5 h. Then the reaction solution was diluted with 150 mL water and extracted with CH_2Cl_2 (100 mL×2). The organic phase was washed with water and brine, dried over anhydrous Na_2SO_4, filtered, and concentrated. The residues were purified over a silica column with petroleum ether (PE)/CH_2Cl_2 (2/5, *v/v*) to afford **DAND** as an orange solid (73.3 mg, yield 62.3%). ^1H NMR (500 MHz, $CDCl_3$) δ 7.99 (s, 1H), 7.63 (d, J = 8.5 Hz, 1H), 7.43 (s, 1H), 7.40 (d, J = 9.7 Hz, 1H), 7.37 (dd, J = 8.6, 2.2 Hz, 1H), 6.67 (d, J = 1.9 Hz, 1H), 6.64 (dd, J = 9.7, 1.9 Hz, 1H),

2.41 (t, J = 7.5 Hz, 2H), 1.79 – 1.71 (m, 2H), 1.55 (s, 6H), 1.41 – 1.25 (m, 12H), 0.88 (t, J = 6.9 Hz, 3H). ^{13}C NMR (125 MHz, $CDCl_3$) δ 187.20, 171.67, 151.63, 147.76, 141.73, 140.54, 138.90, 138.70, 132.85, 131.47, 127.62, 118.46, 116.52, 37.96, 37.41, 32.41, 31.86, 29.42, 29.37, 29.27, 25.42, 22.66, 14.10. HRMS (ESI negative) calced for $[M-H]^-$ 391.2391, found 391.2386 (**Scheme S1, Fig. S3-S5**).

1.3 Incubation condition and analysis method

Spectral characteristics of **DAND** and the fluorescence response of **DAND** toward FAAH were determined in a standard 200 μL buffer containing 125 mM Tris-HCl, 1 mM EDTA, 0.1% EDTA (pH = 8).[1] Firstly, FAAH (the final concentration is 2.5 μg/mL) was preincubated in standard buffer at 37 °C for 3 min, then adding 1 μL **DAND** (final concentration is 10 μM) to initiate reaction and incubated for another 30 min, the concentration of dimethyl sulfoxide in the buffer should not exceed 1% (*v/v*) to avoid the interference of excessive organic solvent on enzyme activity. Finally, 100 μL of ice acetonitrile was added to terminate the reaction. Then the vails were centrifuged at 4 ℃ for 10 minutes at 20000 *g* to obtain supernatants for both fluorescence detection and high-performance liquid chromatography analysis. It is worth noting that the control incubation without enzyme was carried out to confirm that the hydrolysis reaction was FAAH-dependent. For HPLC analysis, the following methods was used: the mobile phase contained 0.03% trifluoroacetic acid water (A) and methanol (B), the flow rate was 0.8 mL/min. and the following gradient conditions were used: 0-5 minutes, 30% B; 5-20 min 30-90% B; 20-30 min 90-100% B; 30-35 min 100% B.

Next, the linear range of FAAH catalyze hydrolysis of DAND from 0-1.75μg/mL was performed by adding different concentration of FAAH. Additionally, the detection limit of FAAH by **DAND** was calculated according to the previous report.[3]

1.4 Acquisition of FAAH enzyme

As the previous study, the vector FAAH-HIS pCDH-PURO for FAAH expression was constructed with primers FAAH_F (5-GATTCTAGAGCTAGCGAATTCGCCACCATGG TGCAGTACGAGCTG-3') and FAAH_R (5-GCCGCGGATCCGATTTAAATTTAGTGG TGGTGGTGGTGGTGCTCGAGGGATGACTGCTTTTCAGGGGTC-3).[1] After sequence verification, the recombinant plasmid was transformed into 293T cells for 6h. Continue to culture cells for 42 hours after changing the transfection solution, the transient 293T cell line with high expression of FAAH was successfully constructed. Then collected transient 293T cell precipitation and obtained the recombinant FAAH according to our previous report [1].

1.5 Exploring the selectivity of DAND toward FAAH

For the isoform screening, **DAND** was incubated with different hydrolases in our standard incubation system, including: CES1B, CES2, HSA, CYP3A4, *β*-GLU, AchE and PGA, Lipase, respectively. The final concentration of all hydrolases was set at 2.5 μg/mL. Next, the chemical inhibition was performed, briefly, different inhibitors including URB597 (FAAH selective inhibitor, 5 nM). KCZ (CYP3As inhibitor, 10 μM), Phenylbutazone (UGT1As inhibitor, 500 μM) and BNPP (CEs general inhibitor, 10 μM), LPA (CES2 selective inhibitor, 10 μM)) and HA (AchE inhibitor, 100 μM)

were added into the incubation system and incubated with FAAH, respectively; Blank solvent instead of inhibitors was added into the assay system which was set as the control group, after pre-incubation, **DAND** was added to initiate the reaction. At last, the inhibition activity was measured by contrast with the control group.

In addition, the stability of **DAND** in various exogenous substrates (GSH, Ser, Trp, Tyr Glu, Gly, Arg, Cys, Lys, Gln, Myristic acid, Glucose) and common ions (Mn^{2+}, Ca^{2+}, Mg^{2+}, Ni^{+}, Zn^{2+}, Sn^{2+}, K^{+}, Cu^{2+}, Fe^{3+}, Na^{+}, Ba^{2+}, Cr^{6+}, NO_3^{-}, CO_3^{2-}, SO_4^{2-}) were evaluated according to the previous description[1]. At last, the influence of pH on the activity of FAAH was investigated. All samples were centrifuged at 20000 *g* and measured their fluorescence response.

1.6 Kinetic Study

Accurate dynamic parameters are crucial to illustrate the catalysis of substrate to enzyme and the basis of probe application. Therefore, we carried out kinetic studies to estimate the kinetic characteristics of **DAND** toward FAAH. Briefly, different concentration of **DAND** (0-50 μM) and FAAH (1 μg/mL) were co-incubated for 30 min, respectively. Incubation time and protein concentration were selected in the linear range. According to the Michaelis-Menton formula (Eq. 1), the K_m and V_{max} values were calculated.

$V=$  ……(1)

V_{max} represents the maximum catalytic velocity; K_m represents the affinity of substrate toward enzyme which is the substrate concentration at the half-maximal velocity.

1.7 Fluorescence Imaging of FAAH in Living Cells

The imaging application of **DAND** at the living cells level was also evaluated. BV2, C6 and U251 cells were cultured in DMEM medium containing 10% fetal bovine serum (FBS) and 1% (*v/v*) antibiotics (penicillin/streptomycin) at 37 °C and 5% CO_2. In order to investigate the biocompatibility of probe in living cells, CCK-8 assay was conducted to evaluate the cytotoxicity of **DAND**. Inoculate 100 μL cell suspension of BV2, C6, U251 cells was seeded in 96-well plates at a concentration of 3.2×10^4/mL, respectively. After adherence, various concentrations of **DAND** (0, 5, 10, 20, 40 μM) were added to the 96-well plate. After another 24 hours incubation, 10 μL CCK8 solution was added to each well of the plate and incubate for about 30 min, finally using SynergyH1 Reader (Bio-Tek) to detect the absorbance of each well at 450 nm and determinate the cell survival rate. For the fluorescence imaging three kinds of cells were seeded on 20 mm glass polylysine-coated confocal cell culture dishes and attached overnight. The next day, changing the culture medium with fresh culture solution containing 20 μM **DAND**, incubated at 37 °C for 30 min, and the control group was incubated with fresh medium containing the same volume of blank solvent, the cell nuclei was stained by Hoechst33342 (5 μg/mL). Additionally, the chemical inhibition group was also performed, URB597 (50 μM) was pre-incubated with BV2 cells and added the probe for the same incubation time. At last, the culture medium was removed and washed the cells with PBS, then imaged on confocal.

1.8 Visual high-throughput screening of FAAH inhibitor from herbal medicines

FAAH is a target for some various diseases including: depression and anxiety [4], obesity [5], CNS disorders [6], inflammation and so on. Herein, we have established a high throughput screening plat for the discovery of FAAH inhibitors. First, 93 kinds of Chinese herbal medicines were weighed, crushed into fine particles with a grinder, sifted through 40 mesh. Weighed each kind of fine particles about 5 g to been ultrasonically extracted with 95% ethanol (50 mL) at room temperature for 60 minutes, repeated extraction for 3 times. Every single extracted solution was leached to remove drug residues. After evaporating solvent, all the dried extractions are dissolved in dimethyl sulfoxide (DMSO) respectively to the concentration of 10 mg/mL, pipette 1 μL into the standard incubation system (containing DMSO < 1%) to determine their inhibitory activity. The control group was incubated with the same volume of dimethyl sulfoxide (DMSO) instead of herbal extraction. After incubating for 30 min with **DAND** (10 μM) at 37 °C, adding 100 μL cold acetonitrile to terminate the reaction. The vials were centrifuged at 20000 *g*, supernatants were transferred into a 96-well plate and imaged by GE Typhoon FLA9500 (The excitation wavelength was Cy5 nm and the emission filter was 670 ± 20 nm). The high-throughput inhibitory heat map of traditional Chinese medicine was obtained. At the same time, all samples were also detected by SynergyH1 reader (Bio-Tek). The control group was 100%, and the inhibitory activity of each herbal extraction was calculated.

1.9 Isolation and identification of key inhibitory compound from herbal *Piper nigrum L.* toward FAAH

The total 95% ethanol extract of *Piper nigrum L.* (30 g) was Weighed and suspended with hot water. The water suspension was sequentially extracted with three organic solvents of different polarity in following order: (1) Petroleum (2) Ether acetate (3) n-butanol. Each solvent extraction was evaporated to dryness to determine its inhibitory activity in rat brain S9. The total extracts of ether acetate were separated into 11 fractions by high performance liquid chromatography (mobile phase: 10% acetonitrile + 90% trifluoroacetic acid water (A) and methanol (B)), flow rate: 10 mL/min. The following condition was adopted: 0-10 min 40% A; 10-20 min 40%-30% A; 20-40 min 30%-10% A; 40-50 min 10% A. All fractions were collected and evaluated their inhibitory activity by the aforementioned fluorescent analysis method. After the screening, Fr. 3 exhibited considerable inhibition activity toward FAAH, next, the active compound (**PN-F3**) was further isolated using HPLC (Isochromatic conditions methanol: trifluoroacetic acid water = 45:55, the flow rate was set at 1.0 mL/min) and the structure of **PN-F3** was identified using NMR analysis.

1.10 Chemical structural modification of Piperine

After a systematic analysis, a series of Piperine derivatives were designed and synthesized. The detailed method for the synthesis was added in the supporting information 2.1 Section.

1.11 Inhibition kinetics

The inhibition behavior of **11f** was investigated using probe **DAND** (0-20 μM) in the presence of various concentrations of **11f** (0-0.5 μM), and the data were analyzed using Graphpad 8.0 and Michealis-Menten plots was described. Lineweaver-Burk analysis

was conducted to confirm the inhibition types of **11f** against FAAH. According to the slope plots, the K_i value was calculated.

1.12 Molecular docking

The discovery Studio 3.5 was used to perform molecular docking of **11f** within FAAH (PDB code 2vya) [7] downloaded from https://www.rcsb.org. The binding site was defined as a radius of 9.5 Å. The protein structure was processed by removing water molecules, adding hydrogen atoms and applying Charmm forcefield. The ligands were prepared by adding hydrogen atoms and energy minimization. Goldscore protocol was used to assess the score of docking, and the other parameters were set as default.[8]

1.13 The bioactivity of Piperine derivative (11f) in LPS-Induced BV2 activation

BV2 cell line was cultured in DMEM medium, supplemented with 10% FBS (fetal bovine serum) and 1% antibiotics (10 units/mL penicillin; 10 μg/mL streptomycin). Inoculate BV2 cells in 6 cm culture dishes and stimulate it with 200 ng/mL LPS into a state of activation to obtain depression model at the cellular level. For the treatment group **11f** was pre-added into the cells with the final concentration of 20 μM. After a 24 h culture, the expression of COX2 and iNOS as the classic protein in the inflammatory reaction were measured. Briefly, the protein samples were extracted by adding RIPA lysis buffer and then quantitated the protein concentration by BCA assay kit. For western blotting assay, 30 μg protein were separated by electrophoresis based on its molecular weight and cut according to prestained protein marker and transferred from gel to PVDF membrane, then blocked in TBST solution (150 mM NaCl, 10 mM Tris-HCl, pH 7.5, and 0.1% Tween 20) containing 5 % skim milk powder for two hours. Followed by immunoblotted with iNOS, COX2 antibody at dilution of 1:1000 at 4 °C overnight, the membranes were washed with TBST solution and treated with secondary antibody at a dilution of 1:5000. The specific bands were imaged and analyzed by CLiNX GenoSens Touch (Shanghai China). Similar experiments have been carried out at least three times.

2.0 Chemical structural modification of Piperine

2.1 Synthesis

*Synthesis of intermediate **3***

Methyl (*E*)-4-bromobut-2-enoate (1.79 g, 10.00 mmol) was added to Triethyl phosphite (1.90 mL, 11 mmol), and then the mixture was allowed to warm up for 4 hours at 130 ℃. Upon the starting material was consumed completely, the hot reaction suspension was poured into 50 mL water, extracted with dichloromethane (3 × 50 mL). The combined organic layers were washed with saturated aqueous sodium bicarbonate and brine, and then dried over anhydrous sodium sulfate. After removing solvent under reduced pressure to obtain the crude oil. The crude oil was purified by silica gel flash chromatography (dichloromethane/methanol 9:1) as a colorless oil, yield 83%. *Methyl (E)-4-(diethoxyphosphoryl) but-2-enoate (**3a**)* ^{1}H-NMR (400 MHz, $CDCl_3$), δ (ppm): 6.89 (1H, m), 5.97 (1H, ddd, J = 15.5, 5.0, 1.3 Hz), 4.13 (4H, q, J = 6.9 Hz), 3.74 (3H, s), 2.78 (1H, d, J = 7.8 Hz), 2.73 (1H, d, J = 7.8 Hz). (**Fig. S15**)

*Synthesis of intermediate **6***

To a solution of 3, 4-dihydroxybenzaldehyde **4** (3.0 g, 10.0 mmol) and K_2CO_3 (2.76 g, 20.0 mmol) in DMF (16 mL), and 1, 2-dibromoethane **5** (3.76 g, 20.0 mmol)

was dropwise added. The reaction mixture was heated at 90 °C and stirred for 12 h. The hot reaction mixture was poured onto ice and extracted with ethyl acetate (3 × 50 mL). The combined organic layers were washed with saturated aqueous sodium bicarbonate and brine, and then dried over anhydrous sodium sulfate. After removing the solvent under reduced pressure, and purified by silica sel flash chromatography (dichloromethane/methanol 2%) as a light yellow solid, yield 73%. Benzo[*d*][1,3]dioxole-5-carbaldehyde (**6**). ^{1}H-NMR (400 MHz, DMSO-d_6), δ (ppm): 9.81 (1H, s), 7.41 (1H, dd, J = 8.0, 1.5 Hz), 7.33 (1H, d, J = 1.5 Hz), 6.92 (1H, d, J = 8.0 Hz), 6.07 (2H, s); ^{13}C-NMR (100 MHz, $CDCl_3$), δ (ppm): 190.2, 153.1, 148.7, 131.9, 128.6, 108.3, 106.9, 102.1. (**Fig. S16** and **S17**)

Synthesis of intermediate 7

To a solution of intermediate **6** (0.75 g, 5.0 mmol) in THF (15 mL), and LiOH (143.7 mg, 6.0 mmol) was added. The reaction mixture was allowed to reflux for 4 h. After removing the solvent under reduced pressure, the mixture was extracted with dichloromethane (3 × 30 mL). The combined organic layers were washed with saturated aqueous sodium bicarbonate and brine, and then dried over anhydrous sodium sulfate. After removing the solvent under reduced pressure, and purified by silica sel flash chromatography (dichloromethane/methanol 2.5%) as a light yellow solid, yield 90%. Methyl (2E,4E)-5-(benzo[*d*][1,3]dioxol-5-yl)penta-2,4-dienoate (**7**) ^{1}H-NMR (400 MHz, $CDCl_3$), δ (ppm): 7.42 (1H, dd, J = 15.1, 15.2 Hz), 6.99 (1H, d, J = 1.3 Hz), 6.91 (1H, dd, J = 8.1, 1.3 Hz), 6.80 (1H, d, J = 15.4 Hz), 6.78 (1H, d, J = 8.1 Hz), 6.70 (1H, dd, J = 15.4, 15.2 Hz), 5.98 (2H,s), 5.94 (1H, d, J = 15.1 Hz), 3.76 (3H, s); ^{13}C-NMR (100 MHz, $CDCl_3$), δ (ppm): 167.6, 148.6, 148.3, 144.9, 140.2, 130.5, 130.5, 124.5, 122.9, 119.9, 108.5, 105.8, 101.3, 51.4. (**Fig. S18** and **S19**)

*Synthesis of intermediate **8***

The intermediate **7** (0.70 mg, 3.0 mmol) was solved in 1N NaOH (50% methanol, 10 mL), and the reaction mixture was stirred at room temperature for 8 h. After removing the methanol, the aqueous phase was acidified by.1N HCl to pH = 3, and the resulting precipitate was collected by filtration to give the intermediate **8** as a yellow solid, yield 94%. *(2E, 4E)-5-(benzo[d][1,3]dioxol-5-yl)penta-2,4-dienoic acid (**9**)* ^{1}H-NMR (400 MHz, $CDCl_3$), δ (ppm): 12.19 (1H, s), 7.30 (1H, ddd, J = 15.1, 14.5, 6.7 Hz), 7.23 (1H, d, J = 1.3 Hz), 7.00 (1H, dd, J = 8.0, 1.3 Hz), 6.98 (1H, d, J = 2.84 Hz), 6.96 (1H, s), 6.92 (1H, d, J = 8.0 Hz), 6.05 (2H, s), 5.92 (1H, d, J = 15.2 Hz), 1.35 (2H, t, J = 7.1 Hz); ^{13}C-NMR (100 MHz, $CDCl_3$), δ (ppm): 168.1, 148.5, 148.4, 145.1, 140.2, 130.9, 125.3, 123.5, 121.5, 108.9, 106.2, 101.8. (**Fig. S20** and **S21**)

*Synthesis of intermediate **9***

To a solution of intermediate **8** (1.0 g, 2.6 mmol), tert-Butyl 1-piperazinecarboxylate (0.48 g, 2.6 mmol) and DIEA (0.67 g，5.2 mmol) in DMF (15 mL), HATU (0.99 g, 2.6 mmol) was added. The mixture was stirred for 15 h at r.t. and the resulting mixture was diluted with water (50 mL) and extracted with dichloromethane (3 × 50 mL). The combined organic layers were washed with saturated aqueous sodium bicarbonate and brine, and then dried over anhydrous sodium sulfate. After removing the solvent under reduced pressure, and purified by silica sel flash chromatography (dichloromethane/methanol 5-8%) as a light yellow solid. *tert-butyl 4-*

*((2E,4E)-5-(benzo[d][1,3]dioxol-5-yl)penta-2,4-dienoyl)piperazine-1-carboxylate (**9**)* ^{1}H-NMR (400 MHz, DMSO-d_6), δ (ppm): 7.26 (1H, d, J = 14.4, 14.8 Hz), 7.18 (1H, d, J = 1.3 Hz), 6.99 (1H, dd, J = 8.1, 1.6 Hz), 6.93 (1H, d, J = 14.5, 15.0 Hz), 6.92 (1H, d, J = 8.1 Hz), 6.91 (1H, d, J = 14.5, 15.0 Hz), 6.66 (1H, d, J = 15.0 Hz), 6.05 (2H, s), 3.54 (4H, brs), 3.33 (4H, brs), 1.41 (9H, s); ^{13}C-NMR (100 MHz, $CDCl_3$), δ (ppm): 165.0, 154.2, 148.4, 148.3, 142.8, 138.7, 131.2, 125.9, 123.1, 120.6, 109.0, 105.9, 101.7, 79.6, 45.2, 44.0, 43.4, 41.7, 28.5. (**Fig. S22** and **S23**)

*Synthesis of intermediate **10***

To a solution of intermediate ***9*** (0.5 g, 1.3 mmol) in CH_2Cl_2 (10 mL), TEA (10 ml) was added. The mixture was stirred for 3 h at r.t. and the solvent was removed under reduced pressure. Water (50 mL) was added and acidified by1 N NaOH to pH = 10, extracted with dichloromethane (3 × 50 mL). The combined organic layers were washed with saturated aqueous sodium bicarbonate and brine, and then dried over anhydrous sodium sulfate. After removing the solvent under reduced pressure, and purified by silica sel flash chromatography (dichloromethane/methanol 10-15%) as a white solid. *(2E,4E)-5-(benzo[d][1,3]dioxol-5-yl)-1-(piperazin-1-yl)penta-2,4-dien-1-one (**10**)* ^{1}H-NMR (400 MHz, DMSO-d_6), δ (ppm): 7.22 (1H, d, J = 14.4, 14.8 Hz), 7.17 (1H, d, J = 1.3 Hz), 6.99 (1H, dd, J = 8.1, 1.6 Hz), 6.93 (1H, d, J = 14.5, 15.0 Hz), 6.92 (1H, d, J = 8.1 Hz), 6.91 (1H, d, J = 14.5, 15.0 Hz), 6.66 (1H, d, J = 15.0 Hz), 6.05 (2H, s), 3.47 (4H, brs), 2.66 (4H, brs); ^{13}C-NMR (100 MHz, DMSO-d_6), δ (ppm): 164.3, 147.9, 147.7, 141.8, 137.8, 130.8, 125.6, 122.5, 120.5, 108.5, 105.4, 101.3, 46.5, 46.2, 45.5, 42.7. (**Fig. S24** and **S25**)

Synthesis of intermediate ***11a-i***

To a solution of intermediate **10** (100 mg, 0.35 mmol) in CH_2Cl_2 (8 mL), isocyanate derivatives (0.35 mmol) and DIEA (115.0 μL, 0.7 mmol) were added. The mixture was stirred for 5 h at r.t. and the resulting mixture was diluted with water (20 mL) and extracted with dichloromethane (3 × 30 mL). The combined organic layers were washed with saturated aqueous sodium bicarbonate and brine, and then dried over anhydrous sodium sulfate. After removing the solvent under reduced pressure, and purified by silica sel flash chromatography (dichloromethane/methanol 5-10%) as a light yellow solid.

*4-((2E,4E)-5-(benzo[d][1,3]dioxol-5-yl)penta-2,4-dienoyl)-N-(p-tolyl)piperazine-1-carboxamide (**11a**)* Light yellow solid, yield 75%. ^{1}H-NMR (400 MHz, DMSO-d_6), δ (ppm): 8.49 (1H, s), 7.34 (2H, d, J = 8.3 Hz), 7.27 (1H, dd, J = 14.4, 14.5 Hz), 7.18 (1H, d, J = 1.7 Hz), 7.04 (2H, d, J = 8.3 Hz), 6.99 (1H, dd, J = 7.8, 1.7 Hz), 6.97 (1H, dd, J = 14.7, 15.0 Hz), 6.92 (1H, d, J = 7.8 Hz), 6.91 (1H, d, J = 15.0 Hz), 6.71 (1H, d, J = 14.7 Hz), 6.05 (2H, s), 3.60 (4H, brs), 3.47 (4H, brs), 2.22 (3H, s); ^{13}C-NMR (100 MHz, $CDCl_3$), δ (ppm): 165.1, 155.4, 148.4, 148.3, 142.8, 138.7, 138.2, 131.2, 131.1, 129.2, 129.2, 125.9, 123.1, 120.7, 120.3, 120.3, 109.0, 105.9, 101.7, 45.4, 44.4, 44.0, 41.8, 20.8. (**Fig. S26** and **S27**)

*4-((2E,4E)-5-(benzo[d][1,3]dioxol-5-yl)penta-2,4-dienoyl)-N-(4-chlorophenyl)piperazine-1-carboxamide (**11b**)* Light yellow solid, yield 78%. ^{1}H-NMR (400 MHz, DMSO-d_6), δ (ppm): 8.74 (1H, s), 7.51 (2H, d, J = 8.9 Hz), 7.29 (1H, d, J = 8.9 Hz), 7.27 (1H, d, J = 14.5 Hz), 7.18 (1H, d, J = 1.5 Hz), 6.99 (1H, dd, J = 8.0, 1.5

Hz), 6.97 (1H, dd, *J* = 14.7, 15.0 Hz), 6.92 (1H, d, *J* = 8.0 Hz), 6.91 (1H, d, *J* = 15.0 Hz), 6.71 (1H, d, *J* = 14.5 Hz), 6.05 (2H, s), 3.60 (4H, brs), 3.49 (4H, brs); ^{13}C-NMR (100 MHz, $CDCl_3$), δ (ppm): 165.1, 155.1, 148.4, 148.3, 142.8, 139.9, 138.7, 131.2, 128.6, 128.6, 125.9, 125.8, 123.1, 121.4, 121.4, 120.6, 109.0, 105.9, 101.7, 45.3, 44.4, 44.1, 41. (**Fig. S27** and **S28**)

*4-((2E,4E)-5-(benzo[d][1,3]dioxol-5-yl)penta-2,4-dienoyl)-N-(2-chlorophenyl)piperazine-1-carboxamide (**11c**)* Light yellow solid, yield 68%. ^{1}H-NMR (400 MHz, DMSO-d_6), δ (ppm): 8.29 (1H, dd, *J* = 15.1, 15.2 Hz), 7.49 (1H, dd, *J* = 8.0, 1.5 Hz), 7.45 (1H, dd, *J* = 8.0, 1.5 Hz), 7.31 - 7.25 (2H, m), 7.18 (1H, d, *J* = 1.5 Hz), 7.15 (1H, td, *J* = 7.8, 1.5 Hz), 6.99 (1H, dd, *J* = 8.0, 1.5 Hz), 6.96 (1H, dd, *J* = 15.6, 15.4 Hz), 6.93 (1H, s), 6.91 (1H, t, *J* = 7.4 Hz), 6.71 (1H, d, *J* = 14.5 Hz), 6.05 (2H, s), 3.62 (4H, m), 3.50 (4H, m); ^{13}C-NMR (100 MHz, $CDCl_3$), δ (ppm): 165.1, 155.4, 148.4, 148.3, 142.8, 138.7, 137.0, 131.2, 129.7, 128.7, 127.7, 127.5, 126.2, 125.9, 123.1, 120.7, 109.0, 106.0, 101.7, 45.3, 44.5, 44.1, 41.8. (**Fig. S29** and **S30**)

*4-((2E,4E)-5-(benzo[d][1,3]dioxol-5-yl)penta-2,4-dienoyl)-N-(3,4-dichlorophenyl)piperazine-1-carboxamide (**11d**)* Light yellow solid, yield 86%.^{1}H-NMR (400 MHz, DMSO-d_6), δ (ppm): 8.89 (1H, s), 7.85 (1H, d, *J* = 2.0 Hz), 7.49 - 7.45 (2H, m), 7.28 (1H, d, *J* = 14.5 Hz), 7.18 (1H, s), 6.99 (1H, dd, *J* = 8.0, 1.5 Hz), 6.97 (1H, dd, *J* = 14.7, 15.0 Hz), 6.93 (1H, d, *J* = 8.0 Hz), 6.91 (1H, d, *J* = 15.0 Hz), 6.71 (1H, d, *J* = 15 Hz), 6.05 (2H, s), 3.62 (4H, brs), 3.50 (4H, brs); ^{13}C-NMR (100 MHz, $CDCl_3$), δ (ppm): 165.1, 156.6, 155.4, 154.9, 148.4, 148.3, 142.8, 138.7, 131.2, 127.9, 127.8, 126.6, 125.9, 125.5, 125.4, 124.4, 124.4, 123.1, 120.7, 116.0, 115.8, 109.0, 105.9, 101.7, 45.3, 44.5, 44.1, 41.8. (**Fig. S31** and **S32**)

*4-((2E,4E)-5-(benzo[d][1,3]dioxol-5-yl)penta-2,4-dienoyl)-N-(3,5-dichlorophenyl)piperazine-1-carboxamide (**11e**)* Light yellow solid, yield 71%. ^{1}H-NMR (400 MHz, DMSO-d_6), δ (ppm): 8.94 (1H, s), 7.61 (2H, d, *J* = 1.8 Hz), 7.28 (1H, dd, *J* = 14.5, 14.6 Hz), 7.18 (1H, d, *J* = 1.8 Hz), 7.12 (1H, d, *J* = 1.5 Hz), 6.99 (1H, dd, *J* = 8.0, 1.5 Hz), 6.97 (1H, dd, *J* = 14.7, 15.0 Hz), 6.93 (1H, d, *J* = 8.0 Hz), 6.91 (1H, d, *J* = 15.0 Hz), 6.71 (1H, d, *J* = 15 Hz), 6.05 (2H, s), 3.62 (4H, brs), 3.50 (4H, brs); ^{13}C-NMR (100 MHz, $CDCl_3$), δ (ppm): 165.1, 154.6, 148.4, 148.3, 143.5, 142.8, 138.7, 134.1, 134.1, 131.2, 125.9, 123.1, 121.1, 120.6, 117.6, 117.6, 109.0, 105.9, 101.7, 45.2, 44.4, 44.0, 41.7. (**Fig. S33** and **S34**)

*4-((2E,4E)-5-(benzo[d][1,3]dioxol-5-yl)penta-2,4-dienoyl)-N-(2-fluorophenyl)piperazine-1-carboxamide (**11f**)* Light yellow solid, yield 88%. ^{1}H-NMR (400 MHz, DMSO-d_6), δ (ppm): 8.39 (1H, s), 7.44 (1H, m), 7.27 (1H, dd, *J* = 14.6, 15.0 Hz), 7.18 (2H, m), 7.11 (2H, m), 6.99 (1H, dd, *J* = 8.0, 1.5 Hz), 6.97 (1H, dd, *J* = 14.7, 15.0 Hz), 6.93 (1H, d, *J* = 8.0 Hz), 6.91 (1H, d, *J* = 15.0 Hz), 6.71 (1H, d, *J* = 15.0 Hz), 6.05 (2H, s), 3.61 (4H, brs), 3.48 (4H, brs); ^{13}C-NMR (100 MHz, $CDCl_3$), δ (ppm): 165.1, 156.7, 155.4, 154.8, 148.4, 148.3, 142.8, 138.7, 131.2, 127.9, 127.9, 126.6, 126.6, 125.9, 125.5, 125.5, 124.5, 124.4, 123.1, 120.7, 116.0, 115.8, 109.0, 105.9, 101.7, 45.3, 44.6, 44.1, 41.8. (**Fig. S35** and **S36**)

*4-((2E,4E)-5-(benzo[d][1,3]dioxol-5-yl)penta-2,4-dienoyl)-N-(3-fluorophenyl)piperazine-1-carboxamide (**11g**)* Light yellow solid, yield 78%. ^{1}H-NMR (400 MHz, DMSO-d_6), δ (ppm): 7.43 (1H, dd, *J* = 14.5, 15.0 Hz), 7.33 - 7.31 (2H, m),

6.99 - 6.96 (3H, m), 6.89 (1H, d, J = 8.0 Hz), 6.97 – 6.70 (4H, m), 6.37 (1H, d, J = 14.6 Hz), 5.97 (2H, s), 4.19 (2H, m), 3.71 (4H, brs), 3.56 (4H, brs); ^{13}C-NMR (100 MHz, $CDCl_3$), δ(ppm): 165.9, 159.8, 158.3, 155.2, 155.2, 155.1, 148.4, 148.2, 144.1, 139.7, 139.6, 134.7, 134.72, 130.6, 124.7, 124.7, 122.8, 122.4, 122.4, 122.3, 122.3, 122.3, 118.4, 115.6, 115.6, 115.5, 115.4, 115.4, 108.5, 105.7, 101.4, 45.4, 44.1, 43.4, 41.4. (**Fig. S37** and **S38**)

*4-((2E,4E)-5-(benzo[d][1,3]dioxol-5-yl)penta-2,4-dienoyl)-N-(4-fluorophenyl)piperazine-1-carboxamide (**11h**)* Light yellow solid, yield 74%. ^{1}H-NMR (400 MHz, DMSO-d_6), δ (ppm): 7.45 (1H, dd, J = 14.5, 14.6 Hz), 7.31 (1H, dt, J = 11.3, 2.2 Hz), 7.22 (1H, dd, J = 14.4, 14.4 Hz), 7.05 (1H, dd, J = 8.0, 1.3 Hz), 6.99 (1H, d, J = 1.3 Hz), 6.90 (1H, dd, J = 8.2, 1.5 Hz), 6.79 (1H, d, J = 15.5 Hz), 6.78 (1H, d, J = 8.2 Hz), 6.76 - 6.71 (3H, m), 6.38 (1H, d, J = 14.6 Hz), 5.97 (2H, s), 3.73 (4H, m), 3.56 (4H, m); ^{13}C-NMR (100 MHz, $CDCl_3$), δ (ppm): 165.9, 163.8, 162.3, 154.5, 148.4, 148.3, 144.0, 140.5, 140.4, 139.6, 130.6, 129.9, 129.9, 124.8, 122.8, 118.4, 115.1, 115.1, 110.0, 109.9, 108.5, 107.4, 107.2, 105.7, 101.3, 45.4, 44.2, 43.4, 41.3. (**Fig. 39** and **S40**)

*4-((2E,4E)-5-(benzo[d][1,3]dioxol-5-yl)penta-2,4-dienoyl)-N-(2,4-difluorophenyl)piperazine-1-carboxamide (**11i**)* Light yellow solid, yield 74%. ^{1}H-NMR (400 MHz, DMSO-d_6), δ (ppm): 7.96 (1H, m), 7.47 (1H, dd, J = 14.5, 14.6 Hz), 6.99 (1H, d, J = 1.5 Hz), 6.91 (1H, dd, J = 8.0, 1.5 Hz), 6.87 – 6.72 (5H, m), 6.47 (1H, d, J = 2.8 Hz), 6.38 (1H, d, J = 14.6 Hz), 5.98 (2H, s), 3.76 (4H, m), 3.58 (4H, m); ^{13}C-NMR (100 MHz, $CDCl_3$), δ (ppm): 165.8, 159.0, 158.9, 157.4, 157.3, 154.3, 153.6, 153.5, 152.0, 151.9, 148.4, 148.3, 144.0, 139.6, 130.7, 124.8, 123.3, 123.3, 123.3, 123.2, 123.1, 123.1, 123.1, 123.1, 122.8, 118.5, 111.3, 111.3, 111.2, 111.1, 108.5, 105.7, 103.6, 103.4, 103.4, 103.2, 101.3, 45.2, 44.1, 43.4, 41.3. (**Fig. S41** and **S42**).

Reference

1. X. Tian, T. Liu, L. Li, B. Shao, D. Yao, L. Feng, J. Cui, T. D. James and X. Ma, *Analy. chem.*, 2020, **92**, 9493-9500.
2. Z. Tian, L. Feng, L. Li, X. Tian, J. Cui, H. Zhang, C. Wang, H. Huang, B. Zhang and X. Ma, *Sensors and Actuators B: Chemical*, 2020, **310**, 127872.
3. B. Wu, Y. Lin, B. Li, C. Zhan, F. Zeng and S. Wu, *Analy. chem.*, 2018, **90**, 9359-9365.
4. W. J. Huang, W. W. Chen and X. Zhang, *Mol. Med. Rep.*, 2016, **14**, 2899-2903.
5. G. Balsevich, M. Sticht, N. P. Bowles, A. Singh, T. T. Y. Lee, Z. Li, P. K. Chelikani, F. S. Lee, S. L. Borgland, C. J. Hillard, B. S. McEwen and M. N. Hill, *Proc. Natl. Acad. Sci. U. S. A.*, 2018, **115**, 7605-7610.
6. K. Ahn, D. S. Johnson and B. F. Cravatt, *Expert Opin. Drug Discov.*, 2009, **4**, 763-784.
7. M. Mileni, D. S. Johnson, Z. Wang, D. S. Everdeen, M. Liimatta, B. Pabst, K. Bhattacharya, R. A. Nugent, S. Kamtekar, B. F. Cravatt, K. Ahn and R. C. Stevens, *Proc. Natl. Acad. Sci. U. S. A.*, 2008, **105**, 12820-12824.
8. D. Yao, D. Pan, Y. Zhen, J. Huang, J. Wang, J. Zhang and Z. He, *Pharmacol. Res.*, 2020, **152**, 104605.

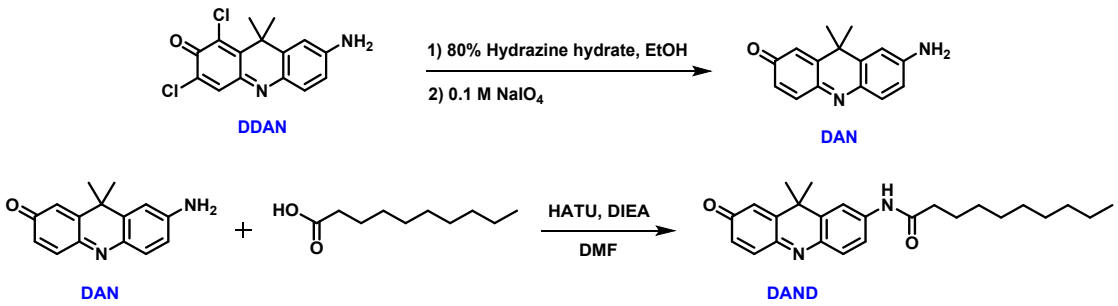

Scheme S1. Synthetic scheme for **DAND**.

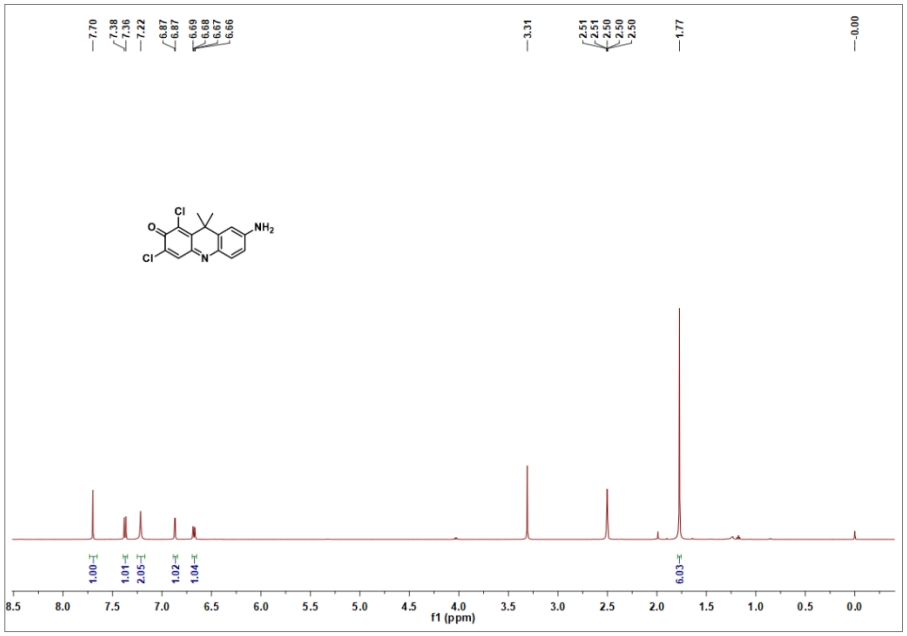

Fig. S1. ^{1}H NMR spectrum of **DDAN** in DMSO-d_6.

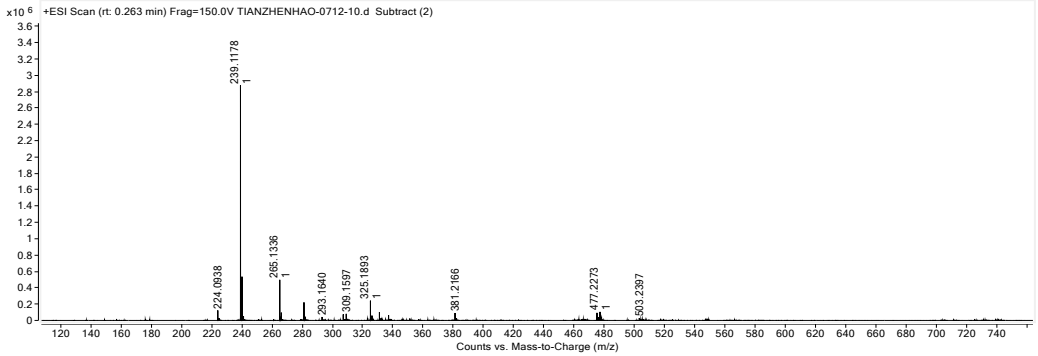

Fig. S2. HRMS of **DAN**.

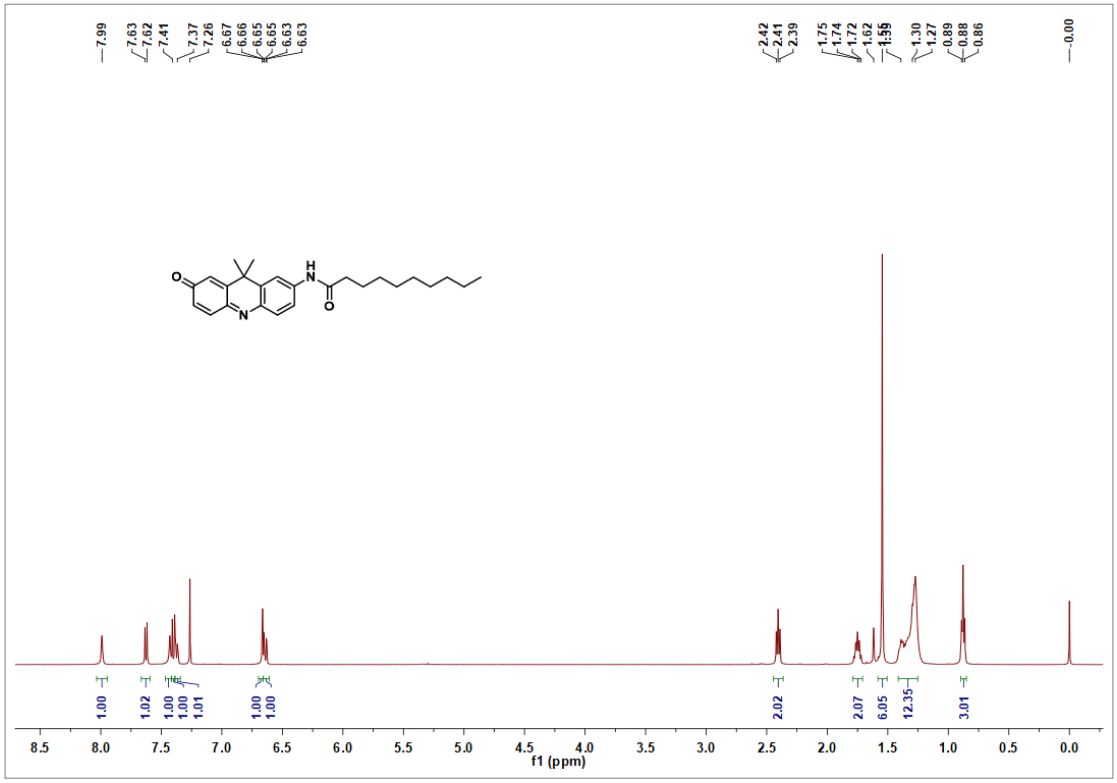

Fig. S3. ^{1}H NMR spectrum of **DAND** in $CDCl_3$.

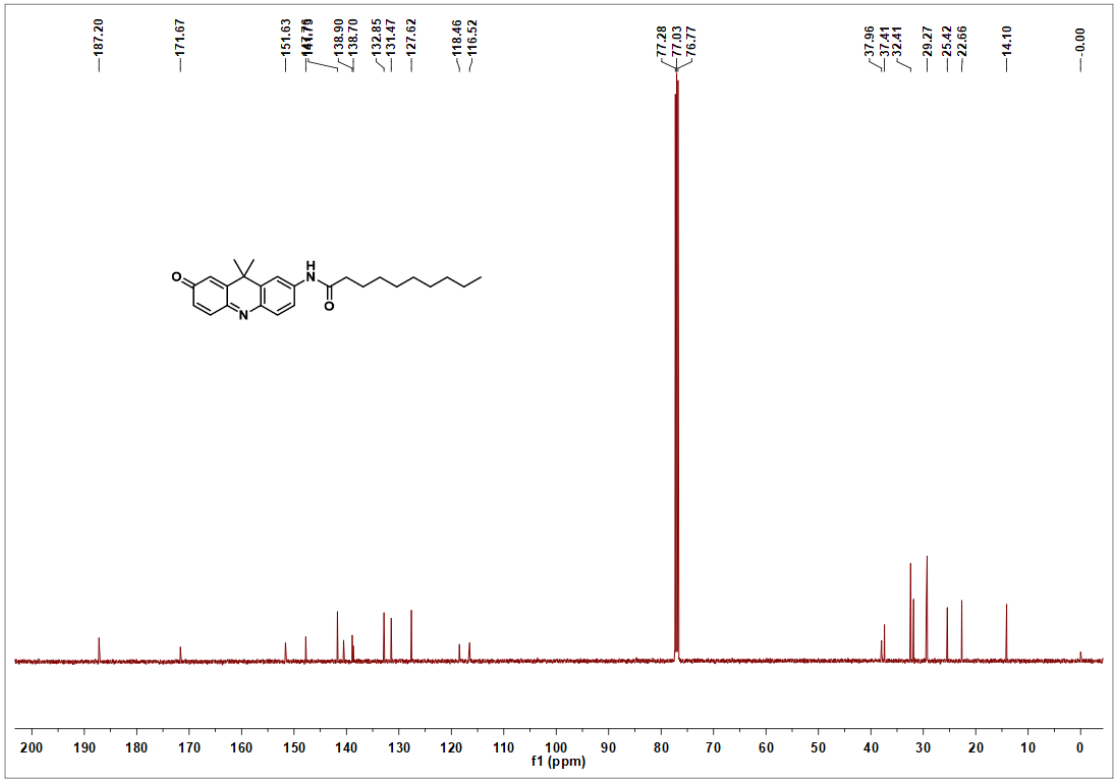

Fig. S4. ^{13}C NMR spectrum of **DAND** in $CDCl_3$.

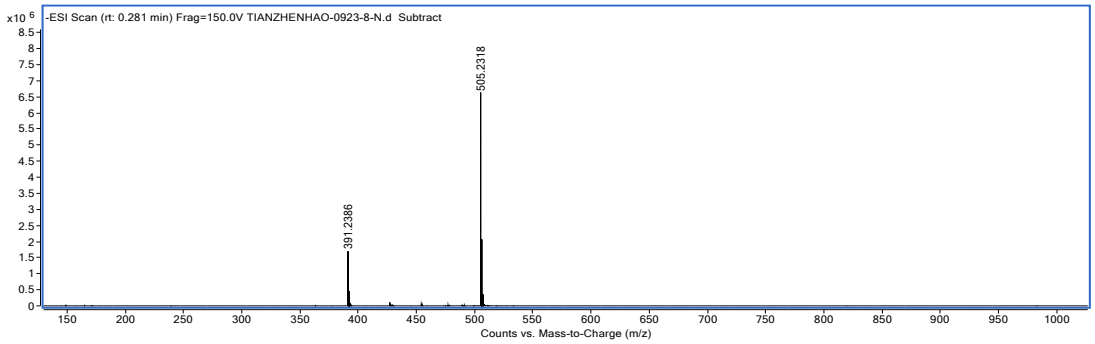

Fig. S5. HRMS of **DAND**.

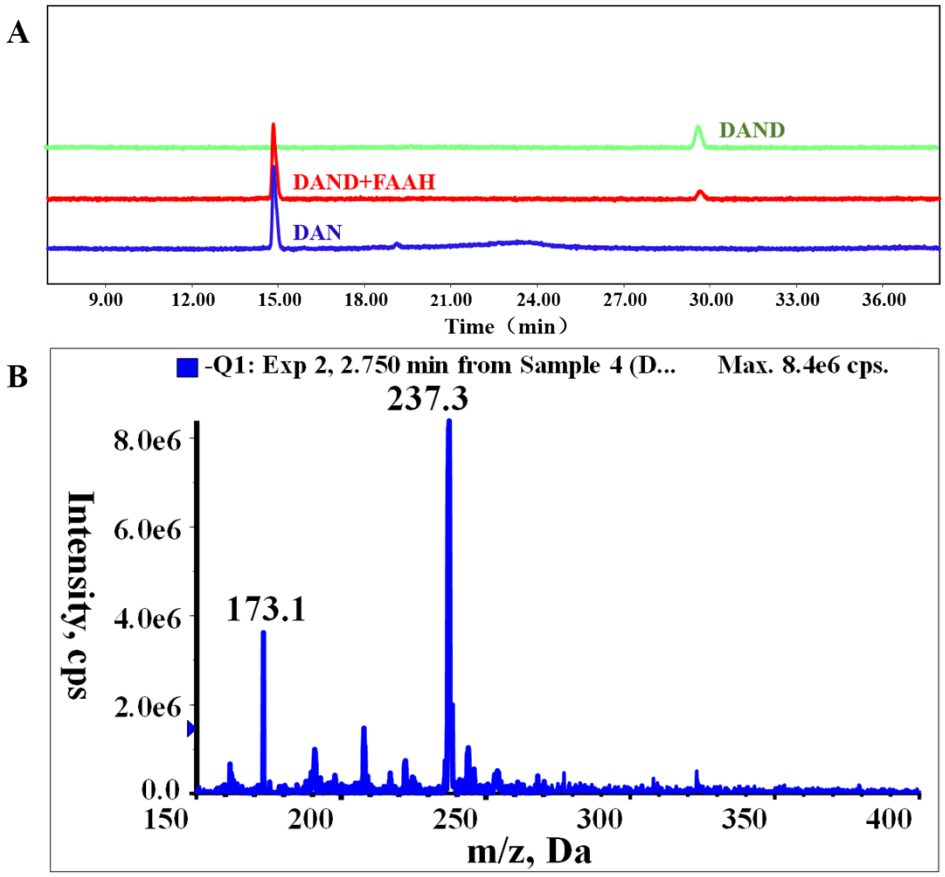

Fig. S6. (A) The HPLC analysis of **DAND** (Green), metabolite **DAN**(Blue), and FAAH mediated **DAND** hydrolysis (Red); (B)The ESI-MS/MS spectrum of metabolite of **DAND** in negative model after incubation in standard system.

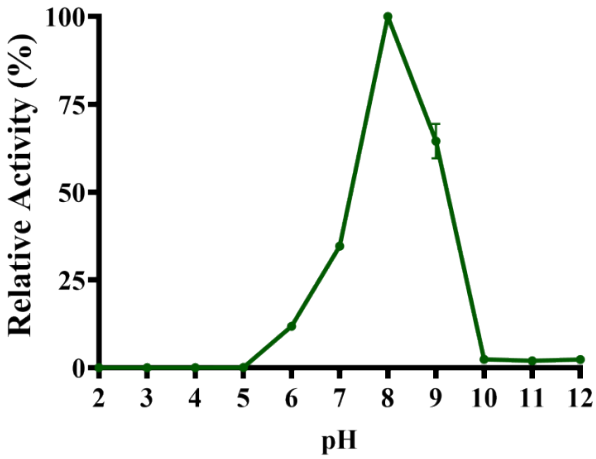

Fig. S7. The influence of pH of incubation system on FAAH metabolism to **DAND**.

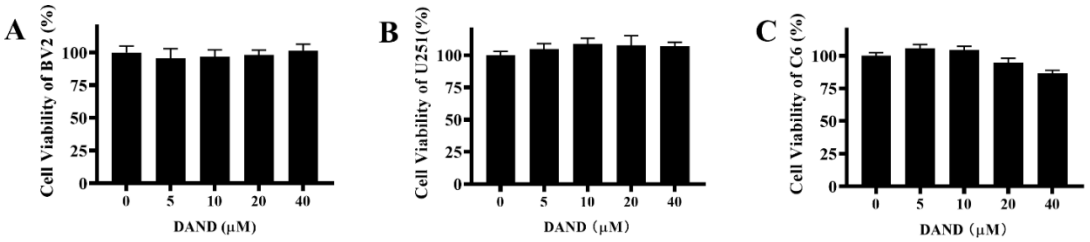

Fig. S8. The cytotoxicity assays of **DAND** in BV2, C6 and U251 cell lines for 24 h, respectively.

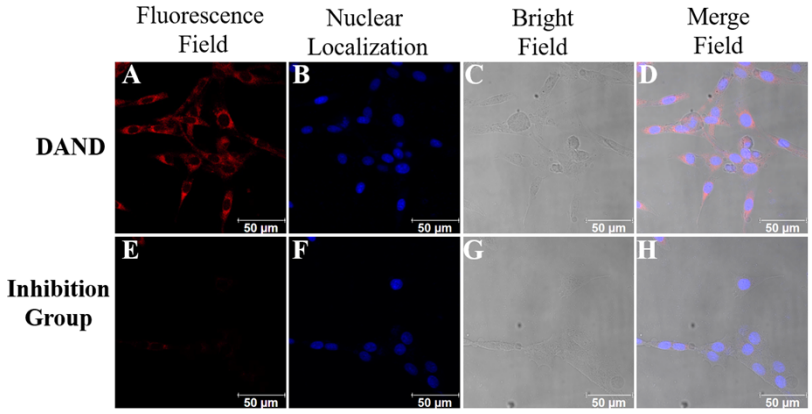

Fig. S9. (A-D) Fluorescence imaging of C6 cells after incubation with **DAND**; (E-H) Fluorescence imaging of FAAH in C6 cells in presence of **DAND** after pre-incubating with FAAH inhibitor URB597. Scale bars 50 μm.

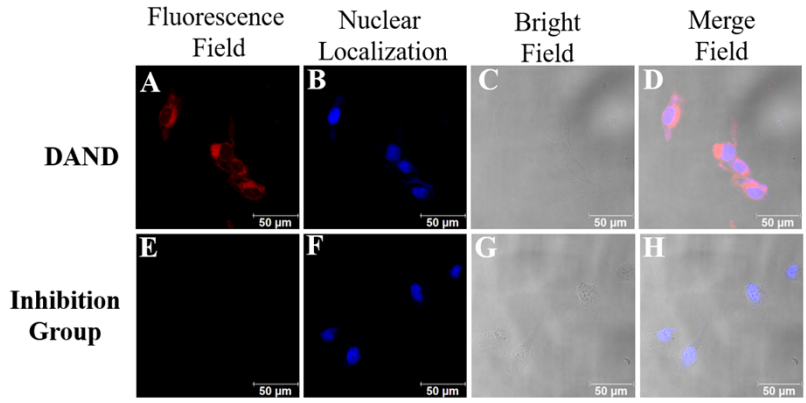

Fig. S10. (A-D) Fluorescence imaging of U251 cells after incubation with **DAND**; (E-H) Fluorescence imaging of FAAH in U251 cells in presence of **DAND** after pre-incubating with FAAH inhibitor URB597. Scale bars 50 μm.

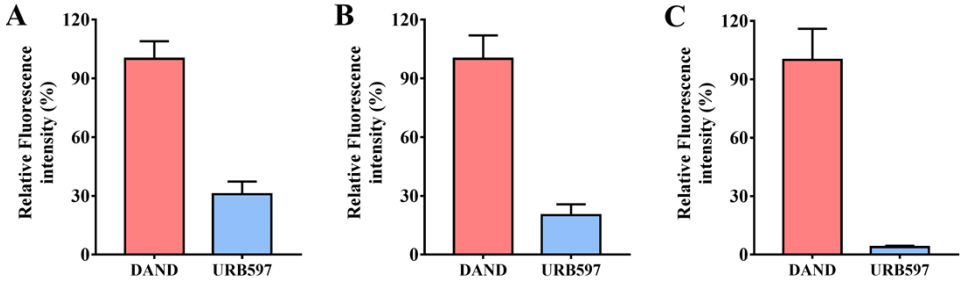

Fig. S11. The quantitative analysis of fluorescence intensity for the FAAH imaging in BV2 (A), C6 (B) and U251 (C) cells, respectively.

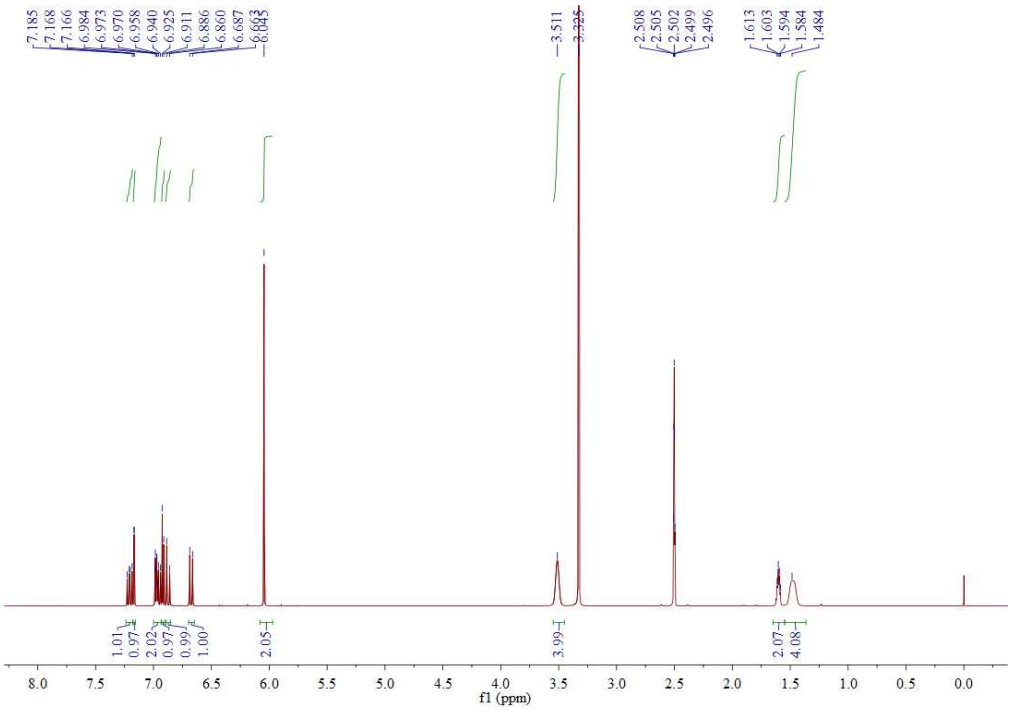

Fig. S12. ^{1}H NMR spectrum of compound PN-F3 (**Piperine)** (DMSO-d_6).

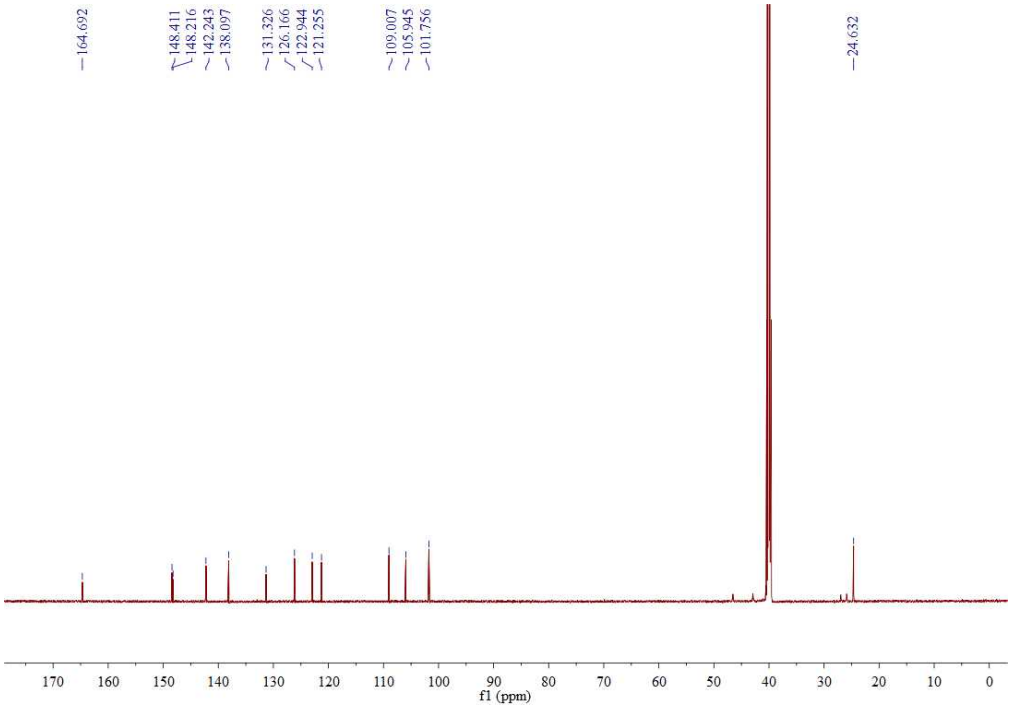

Fig. S13. ^{13}C NMR spectrum of compound PN-F3 (**Piperine**) (DMSO-d_6).

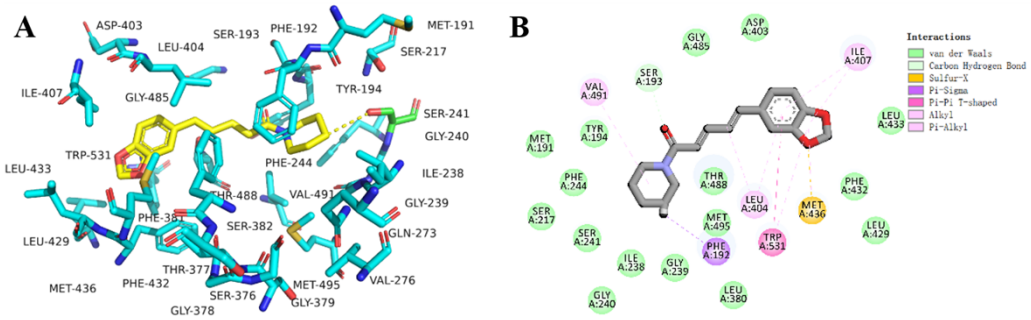

Fig. S14 (A) The detailed interactions between Piperine with FAAH; (B) the 2D interaction of Piperine with FAAH.

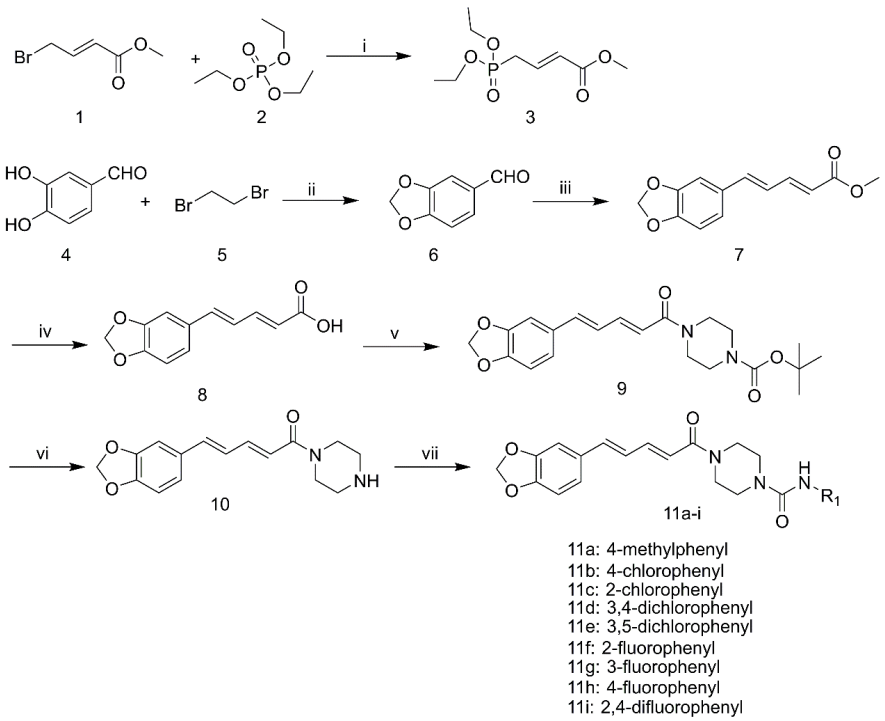

Fig. S15. General synthesis of compounds **11a-i.** Reagents and conditions: (i) 130 ℃, 4 h; (ii) K_2CO_3, DMF, 90 ℃, 12 h; (iii) LiOH, THF, reflux, 4 h; (iv) 1N NaOH (50% methanol); (v) HBTU, DIEA, tert-Butyl 1-piperazinecarboxylate, DMF, r.t.; (vi) CH_2Cl_2/TEA (1:1), r.t.; (vii) isocyanate derivatives, CH_2Cl_2, DIEA, r.t..

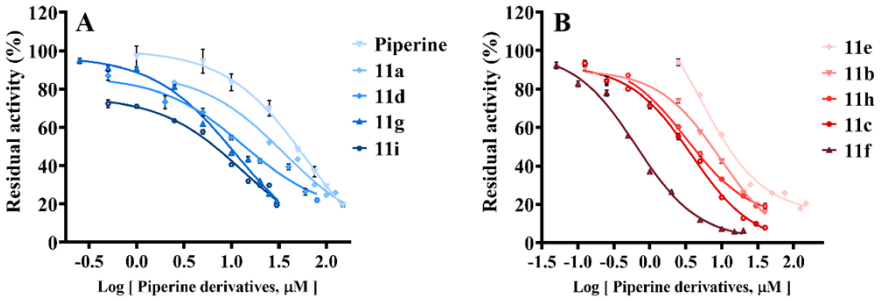

Fig. 16. The inhibition curves of Piperine and its derivatives toward FAAH.

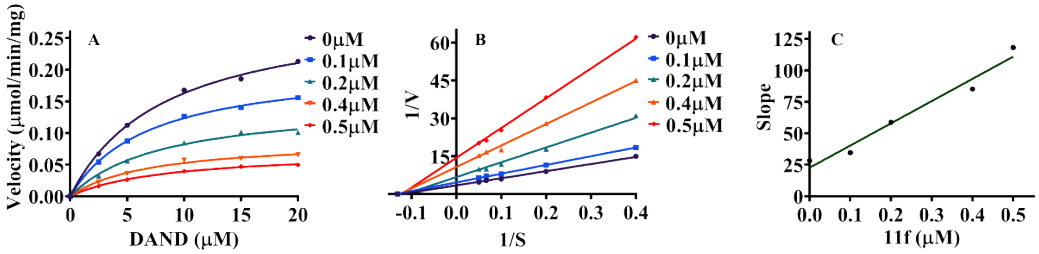

Fig. 17. (A) Michealis-Menten plot of **11f** against FAAH; (B) Lineweaver-Burk plot of **11f** against FAAH; (C) Slope plot of **11f** against FAAH.

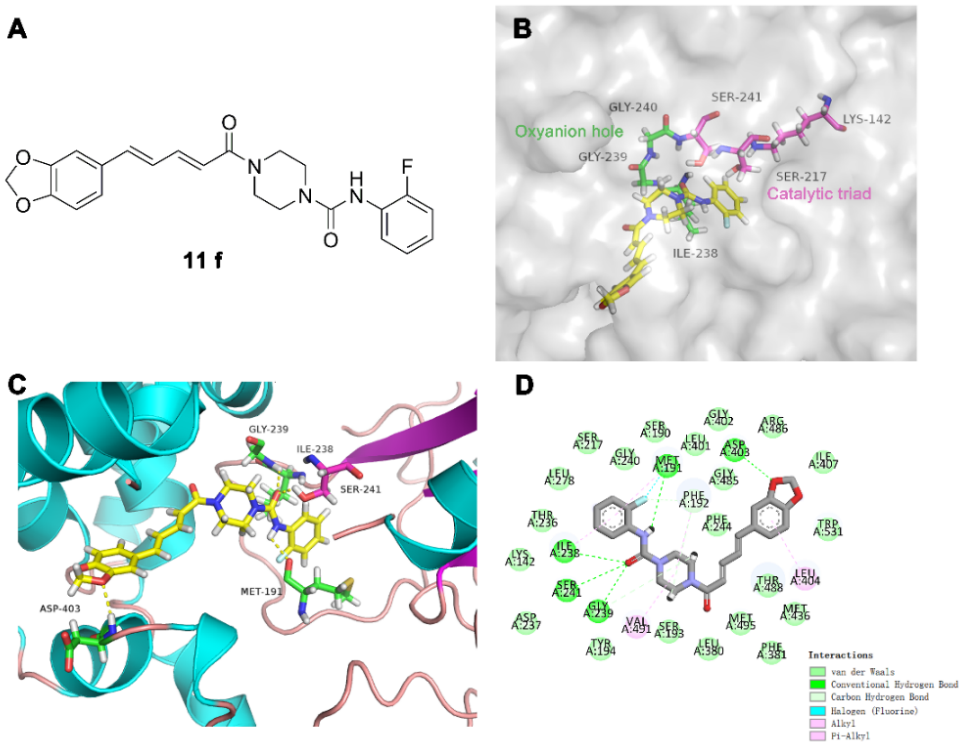

Fig. S18. Molecular docking of **11f** and FAAH. (A) The structure of **11f**; (B) the surface views of **11f**-FAAH complex, the catalytic triad (Ser241-Ser217-Lys142) and oxyanion hole (Ile238, Gly239, and Gly240); (C) the 3D views of **11f**-FAAH; (D) the detailed interactions of **11f**-FAAH.

Table S1. The name of herbal medicines in the screening of FAAH inhibitors.

Herb	Latin name	Herb	Latin name
A4	*Radix Salviae Miltiorrhizae*	**G3**	*Gentiana macrophylla Pall.*
A5	*Cortex Phellodendri*	**G4**	*Herba Ecliptae*
A6	*Radix Scutellariae*	**G5**	*Herba Gynostemmatis Pentaphylli*
A7	*Citrus aurantium L.*	**G6**	*Fructus Malvae*
A8	*Rhizoma Anemarrhenae*	**G7**	*Viola yedoensis Makino*
B1	*Rhizoma Picrorhizae*	**G8**	*Cibotium barometz (L.) J. Sm.*
B2	*Rhizoma Ligustici Chuanxiong*	**H1**	*Fructus Rosae Laevigatae*
B3	*Radix PeuceDANi*	**H2**	*Celosia argentea L.*
B4	*Lignum Sappan*	**H3**	*Cinnamomum wilsonii Gamble*
B5	*Cortex Albiziae*	**H4**	*Dioscorea nipponica Makino*
B6	*Radix Sanguisorbae*	**H5**	*MeLia toosenDAN Sieb.et Zucc.*
B7	*Radix Clematidis*	**H6**	*Gardenia jasminoides Ellis*
B8	*Radix Paeoniae Rubra*	**H7**	*Rhizoma Polygoni Cuspidati*
B9	*Fructus Crataegi*	**H8**	*Semen Armeniacae Amarum*
C2	***Piper nigrum L***	**I1**	*Glaucescent Fissistigma*
C3	*Herba Lycopi*	**I2**	*Radix Platycodonis*
C4	*Semen Sinapis Albae*	**I3**	*Caulis Spatholobi*
C5	*Spica Prunellae*	**I4**	*Herba Menthae Heplocalycis*
C6	*Rhizoma Corydalis*	**I5**	*Herba Schizonepetae*
C7	*Radix Glycyrrhizae*	**I6**	*Gastrodia elata Bl.*
C8	*Semen Arecae*	**I7**	*Radix Panacis Quinquefolii*
D1	*Fructus Forsythiae*	**I8**	*Exocarpium Citri Grandis*
D2	*Radix Angelicae Sinensis*	**J1**	*Pericarpium Citri Reticulatae Viride*
D3	*Radix Angelicae Pubescentis*	**J2**	*Radix Achyranthis Bidentatae*
D4	*Radix Sophorae Flavescentis*	**J3**	*Zingiber officinale Rosc.*
D5	*Flos Carthami*	**J4**	*Herba Cynomorii*
D6	*Typha orientalis Presl*	**J5**	*Rhizoma Coptidis*
D7	*Paeonia lactiflora Pall.*	**J6**	*Caulis Sargentodoxae*
D8	*Cacumen Platycladi*	**J7**	*Myrrha*
E1	*Radix Cynanchi Atrati*	**J8**	*Herba Eupatorii*
E2	*Caulis Bambusae in Taenia*	**K1**	*Radix Angelicae Dahuricae*
E3	*Herba Cirsii*	**K2**	*Perilla frutescens （L.） Britt.*
E4	*Radix Pseudostellariae*	**K3**	*Fructus Liquidambaris*
E5	*Fructus Citri Sarcodactylis*	**K4**	*Rhizoma Alpiniae Officinarum*
E6	*Folium Nelumbinis*	**K5**	*Rhizoma Alismatis*
E7	*Radix Paeoniae Alba*	**K6**	*Pseudobulbus Cremastrae seu Pleiones*
E8	*Spina Gleditsiae*	**K7**	*Dendrobii Herba*
F1	*Cortex Cinnamomi*	**K8**	*Herba Agrimoniae*
F2	*Cortex Lycii*	**L1**	*Typha angustifolia L.*

F3	*Radix Morindae Officinalis*	**L2**	*Herba Ephedrae*
F4	*Nodus Nelumbinis Rhizomatis*	**L3**	*Caulis Sinomenii*
F5	*Illicium difengpi B · N · Changet al*	**L4**	*Cortex Moutan Radicis*
F6	*Cortex Acanthopanax Radicis*	**L5**	*Flos Lonicerae*
F7	*Radix Stephaniae Tetrandrae*	**L6**	*Radix Gentianae*
F8	*Folium Artemisiae Argyi*	**L7**	*Radix Aucklandiae*
G1	*Eriobotrya japonica (Thunb.) Lindl.*	**L8**	*Radix Ginseng Rubra*
G2	*Hemerocallis citrina Baroni*		

Table S2. The FAAH inhibitory activity of compounds **11a-i**.

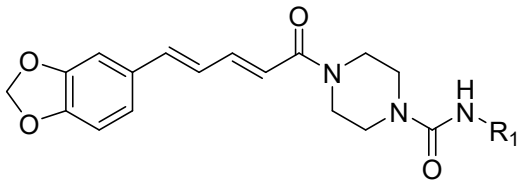

Compound	R^1	Inhibitory activity (IC_{50}, μM)[a]
		FAAH
11a	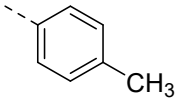	35.76
11b	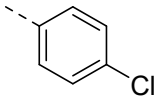	8.36
11c	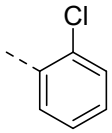	3.79
11d	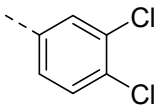	15.79
11e	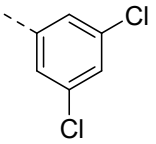	4.19
11f	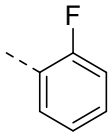	0.65
11g	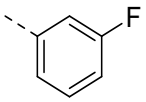	11.18
11h	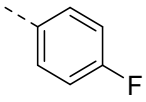	1.79
11i	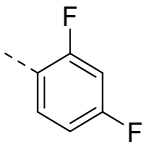	13.24

The NMR data of Piperine derivatives (11a-11i) were added as follows:

1. ^{1}H and ^{13}C NMR of Compounds

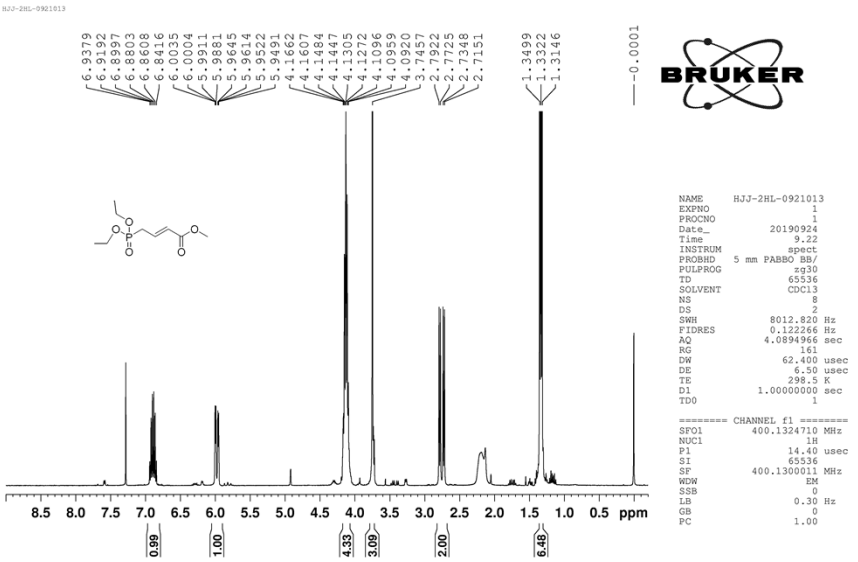

Fig. S19 ^{1}H-NMR spectrum of compound **3**

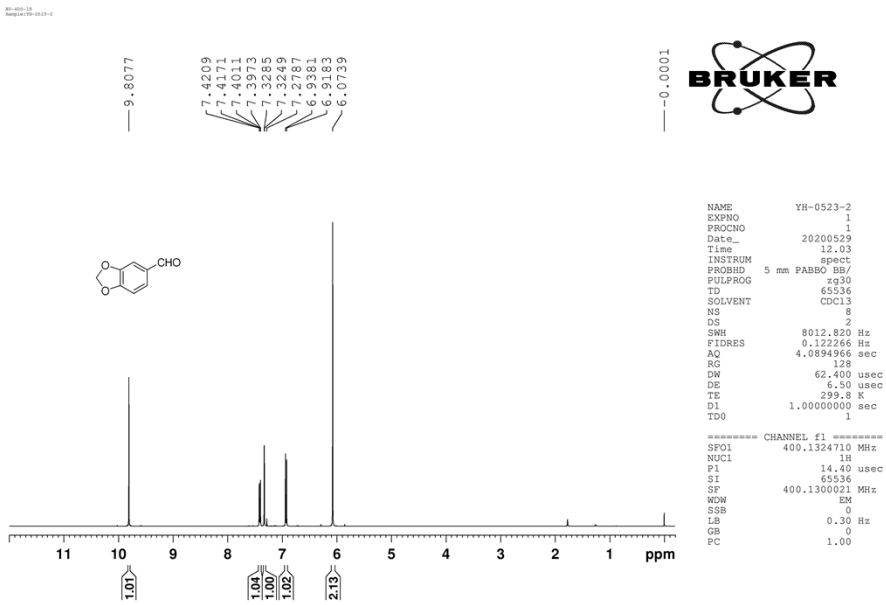

Fig. S20 ^{1}H-NMR spectrum of compound **6**

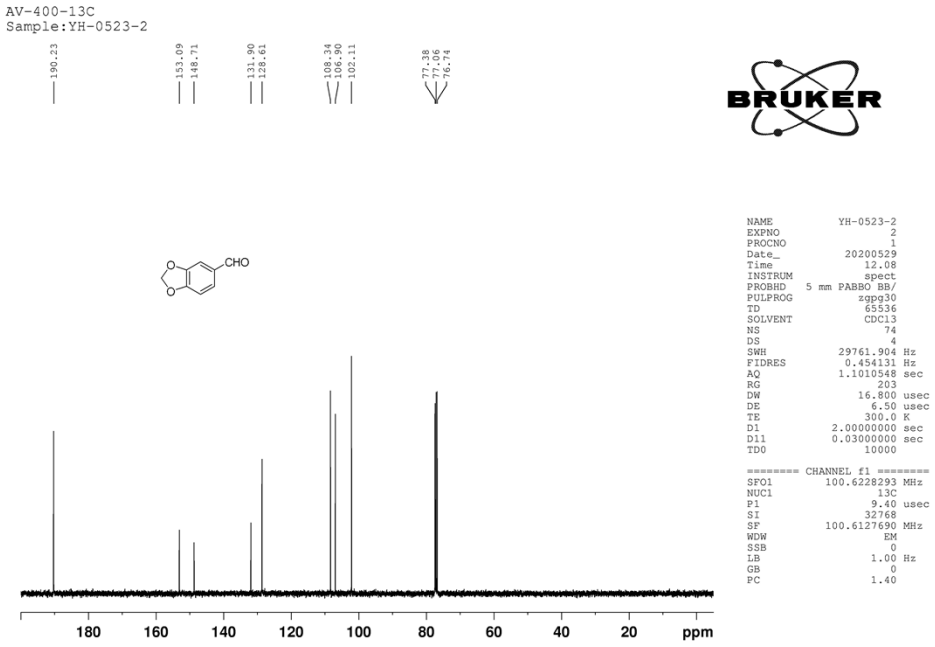

Fig. S21 ^{13}C-NMR spectrum of compound **6**

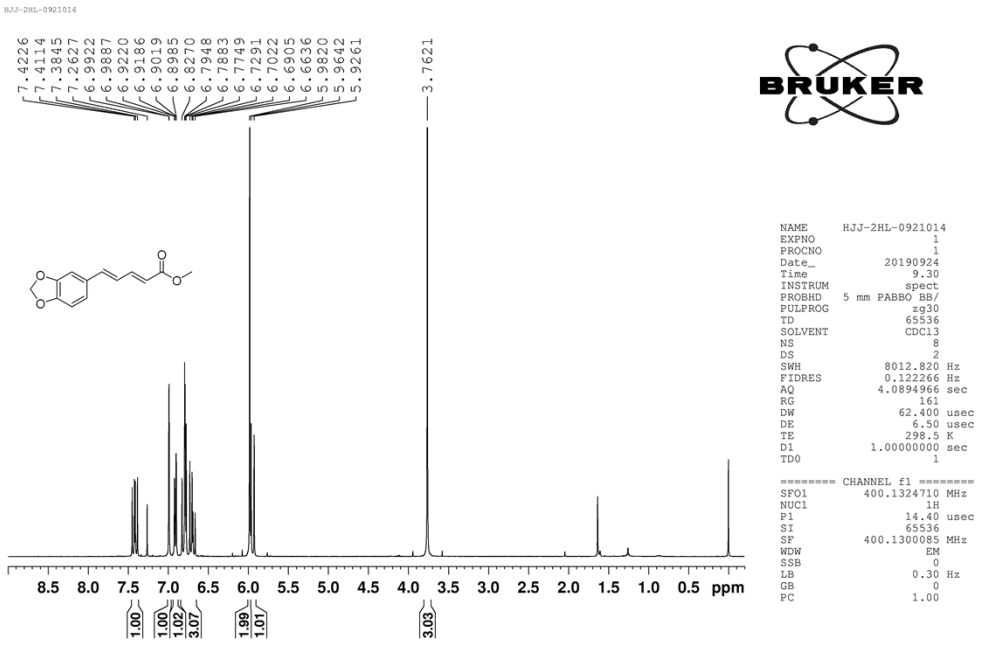

Fig. S22 ^{1}H-NMR spectrum of compound **7**

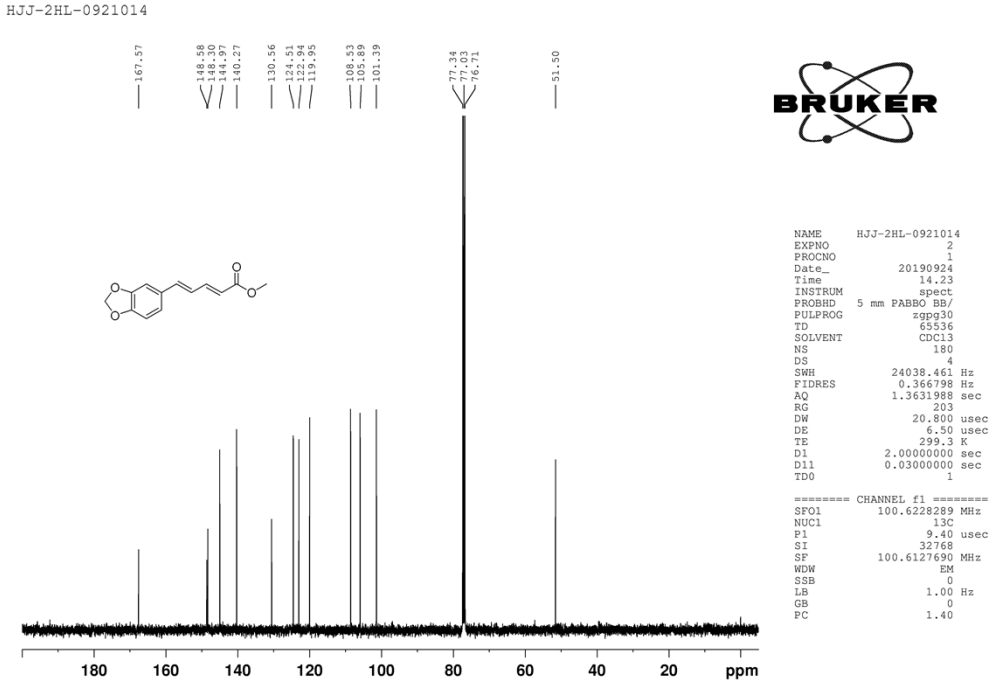

Fig. S23 ^{13}C-NMR spectrum of compound **7**

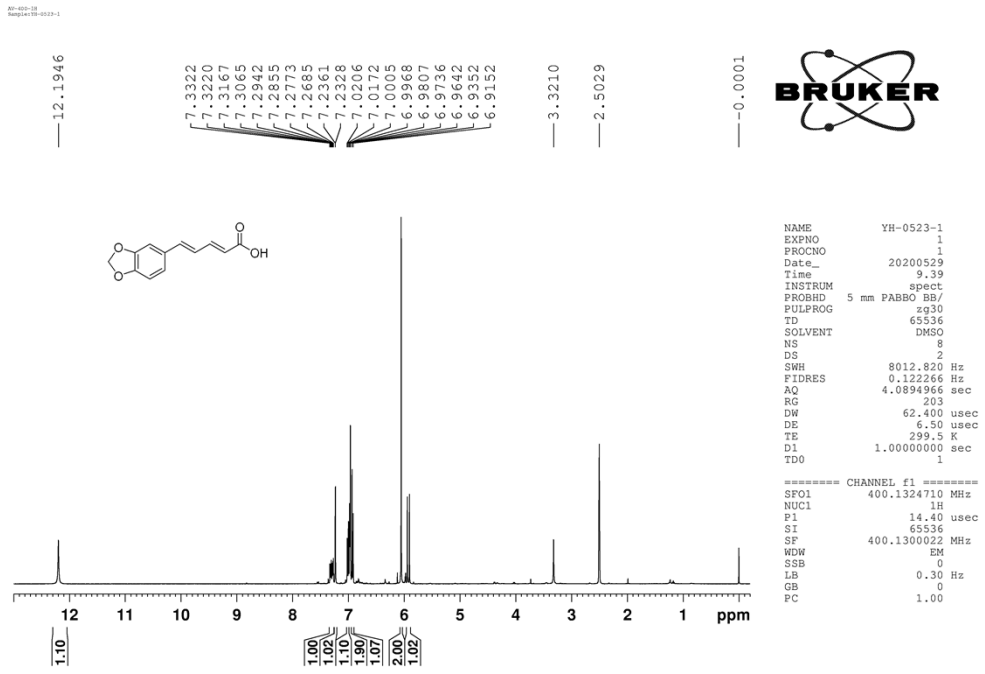

Fig. S24 ^{1}H-NMR spectrum of compound **8**

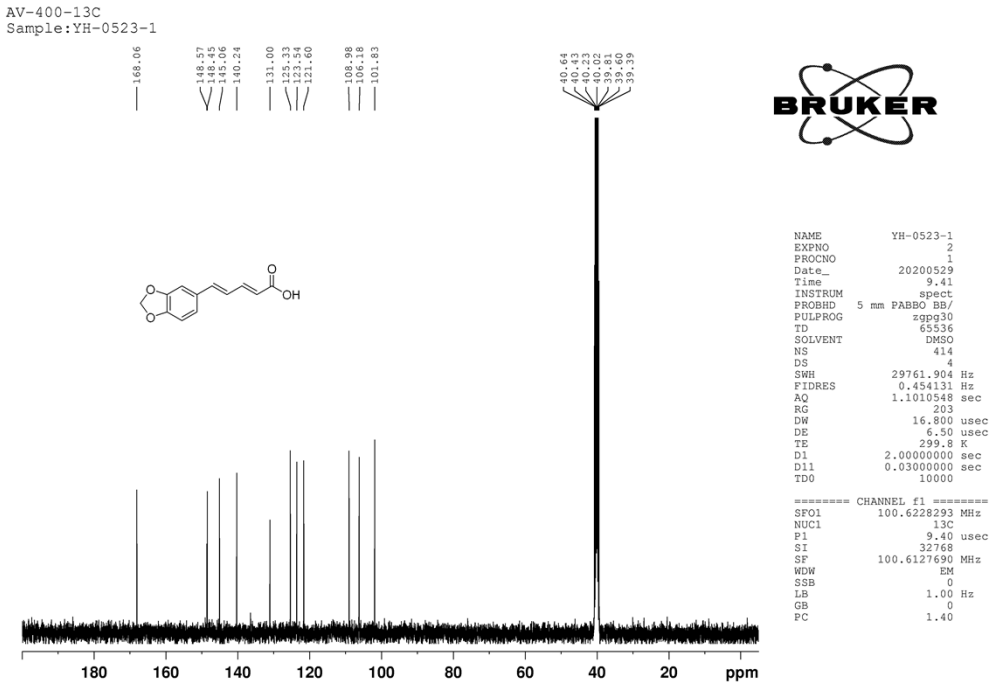

Fig. S25 ^{13}C-NMR spectrum of compound **8**

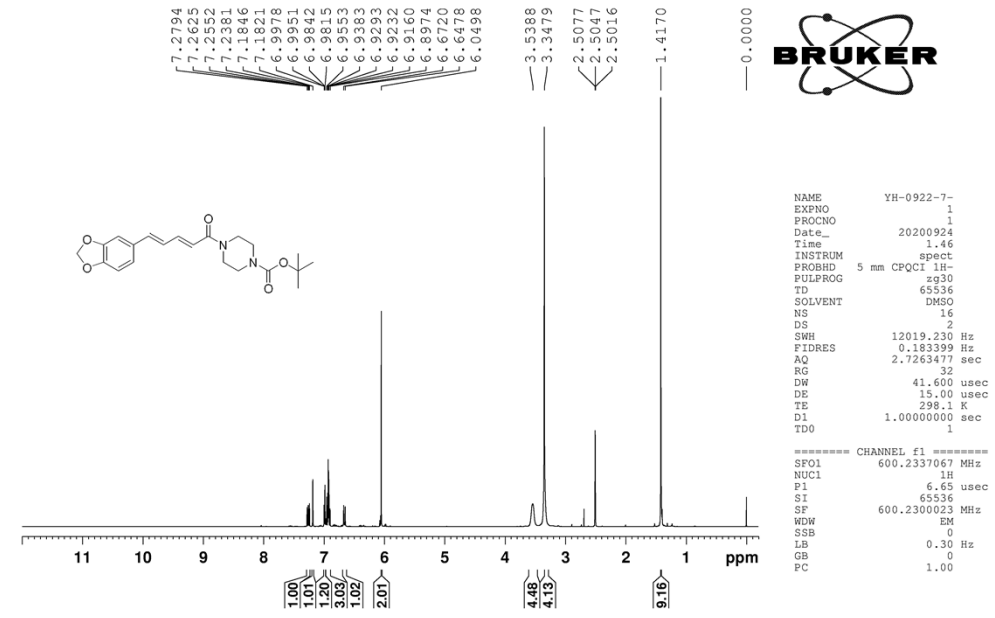

Fig. S26 ^{1}H-NMR spectrum of compound **9**

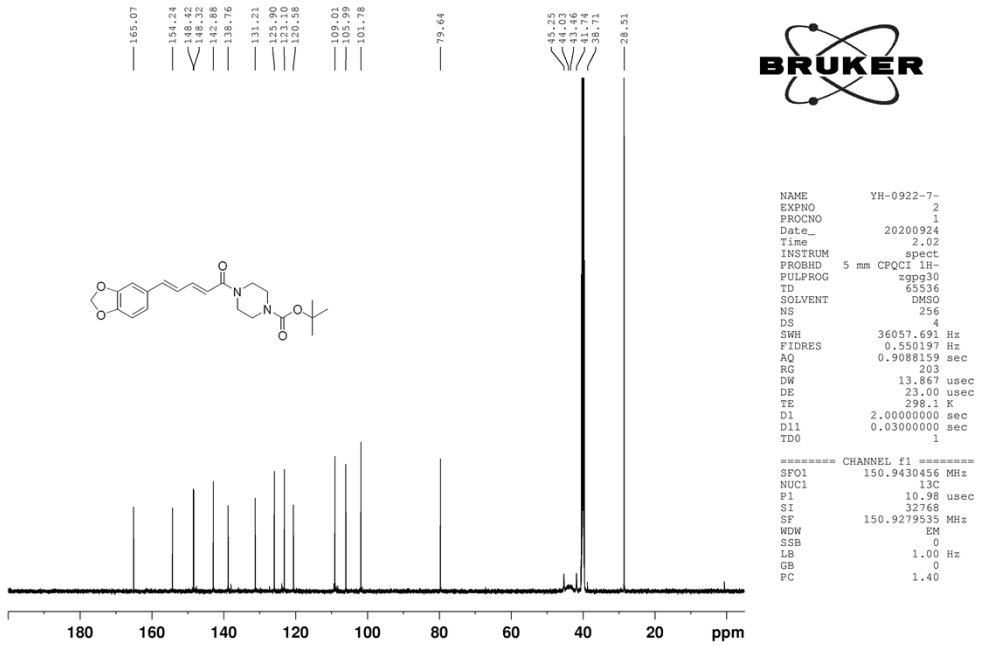

Fig. S27 ^{13}C-NMR spectrum of compound **9**

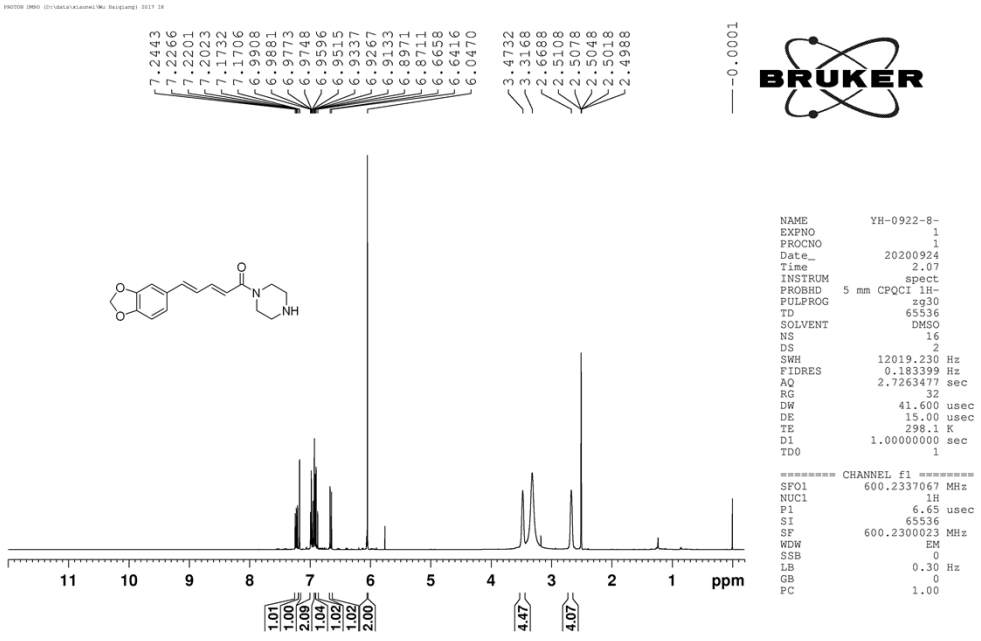

Fig. S28 ^{1}H-NMR spectrum of compound **10**

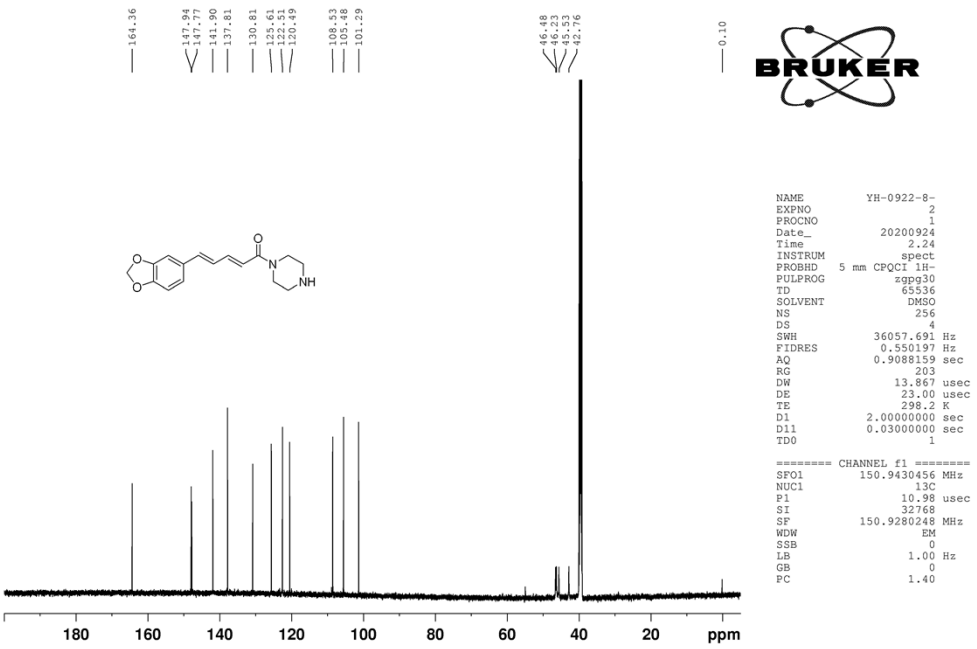

Fig. S29 ^{13}C-NMR spectrum of compound **10**

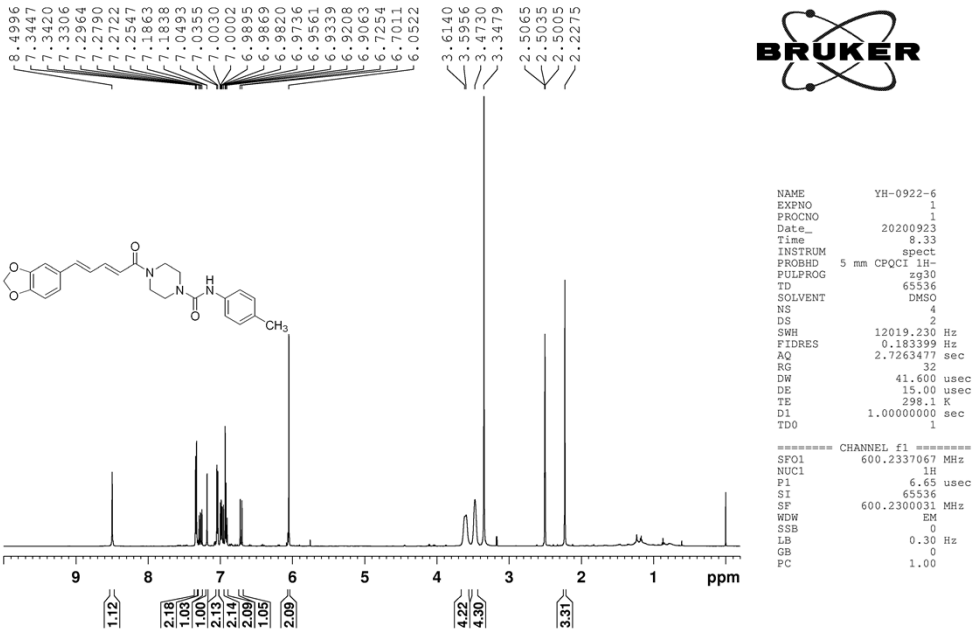

Fig. S30 ^{1}H-NMR spectrum of compound **11a**

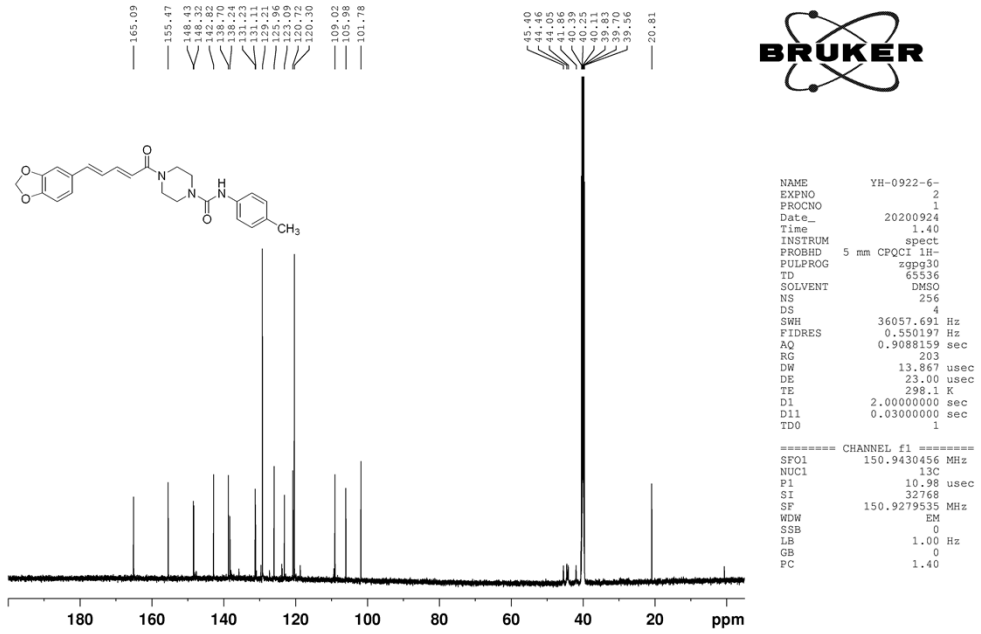

Fig. S31 ^{13}C-NMR spectrum of compound **11a**

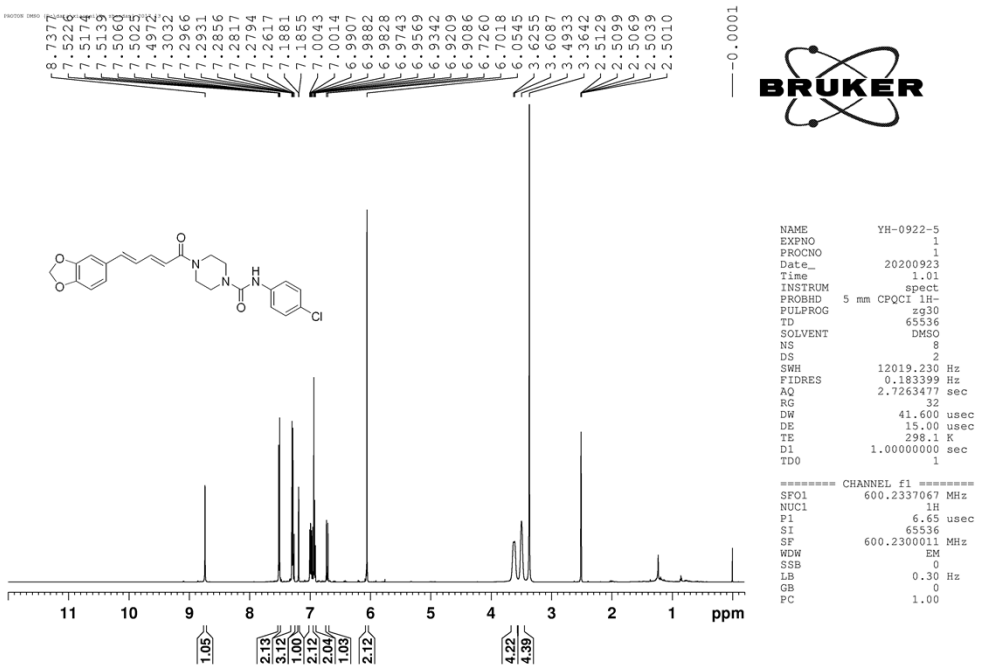

Fig. S32 ^{1}H-NMR spectrum of compound **11b**

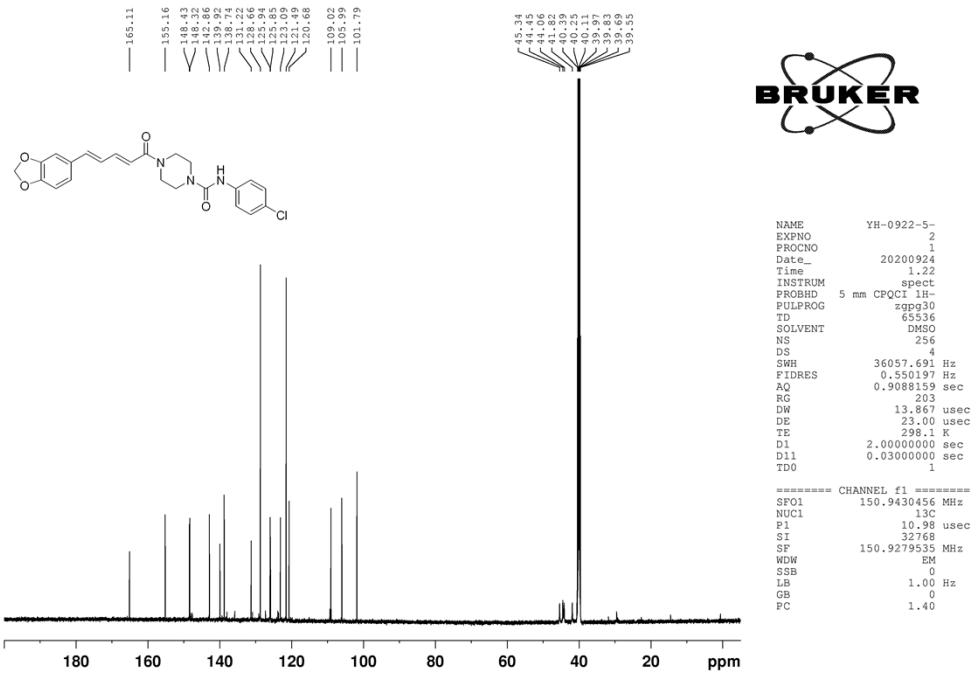

Fig. S33 ^{13}C-NMR spectrum of compound **11b**

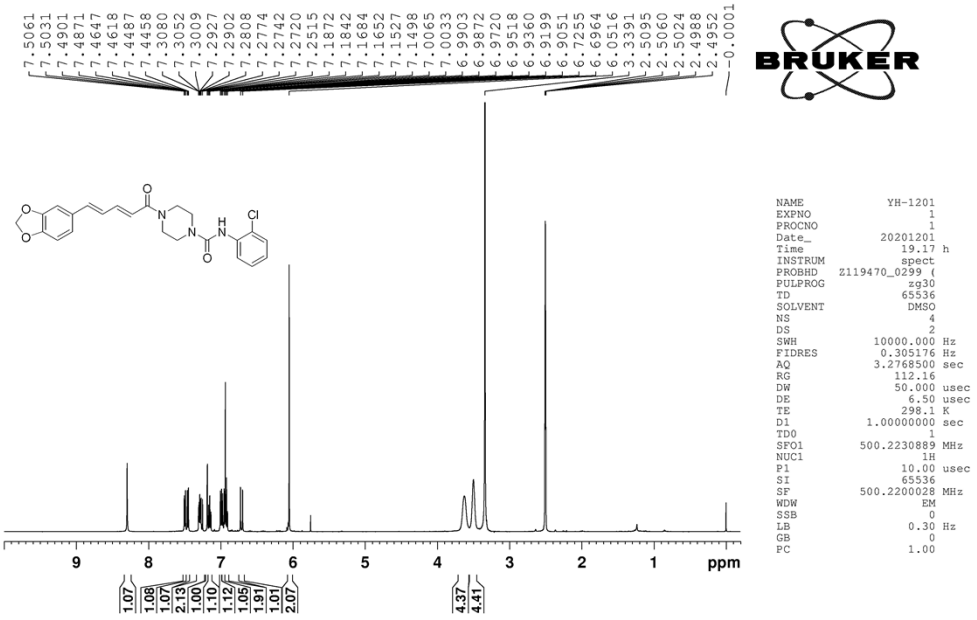

Fig. S34 ^{1}H-NMR spectrum of compound **11c**

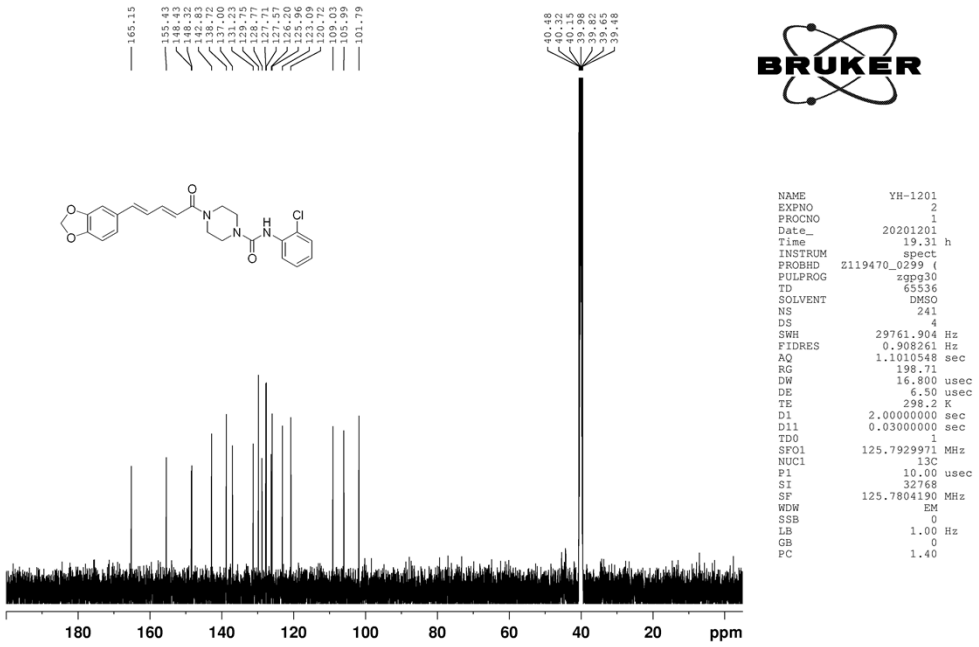

Fig. S35 ^{13}C-NMR spectrum of compound **11c**

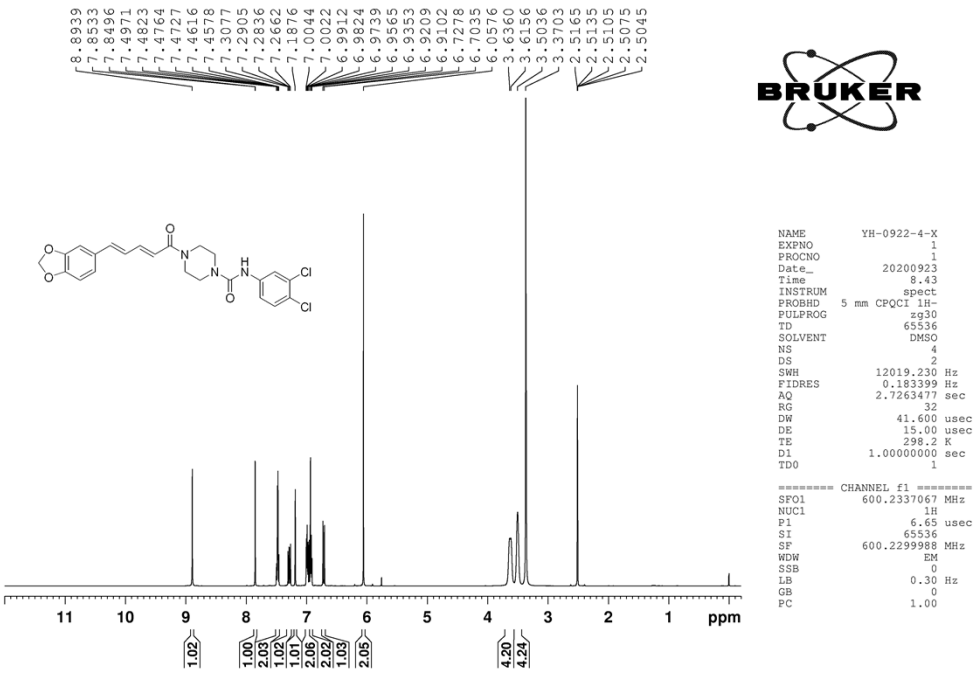

Fig. S36 ^{1}H-NMR spectrum of compound **11d**

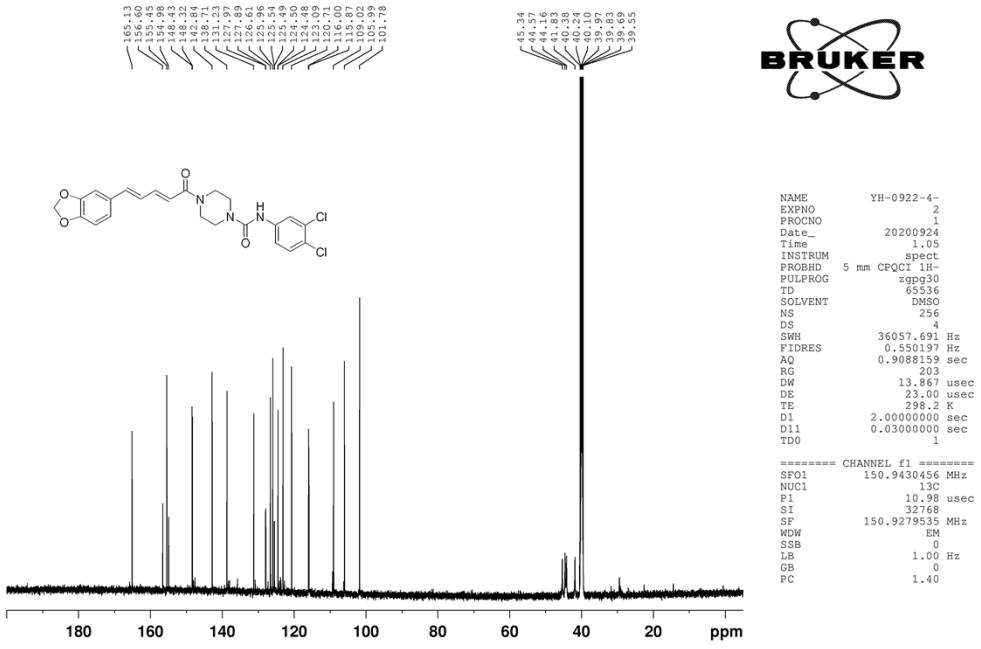

Fig. S37 ^{13}C-NMR spectrum of compound **11d**

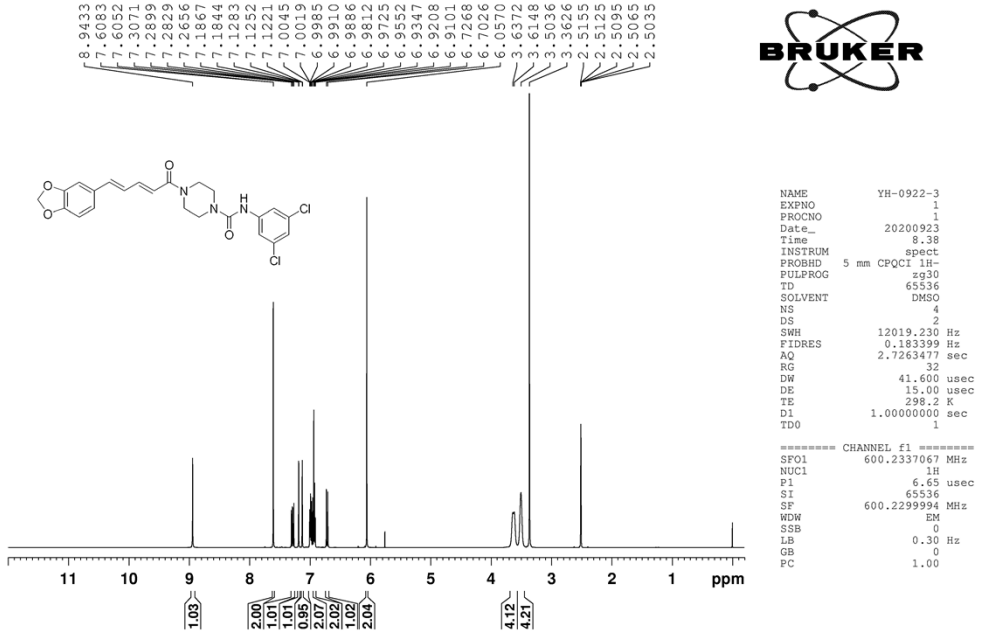

Fig. S38 ^{1}H-NMR spectrum of compound **11e**

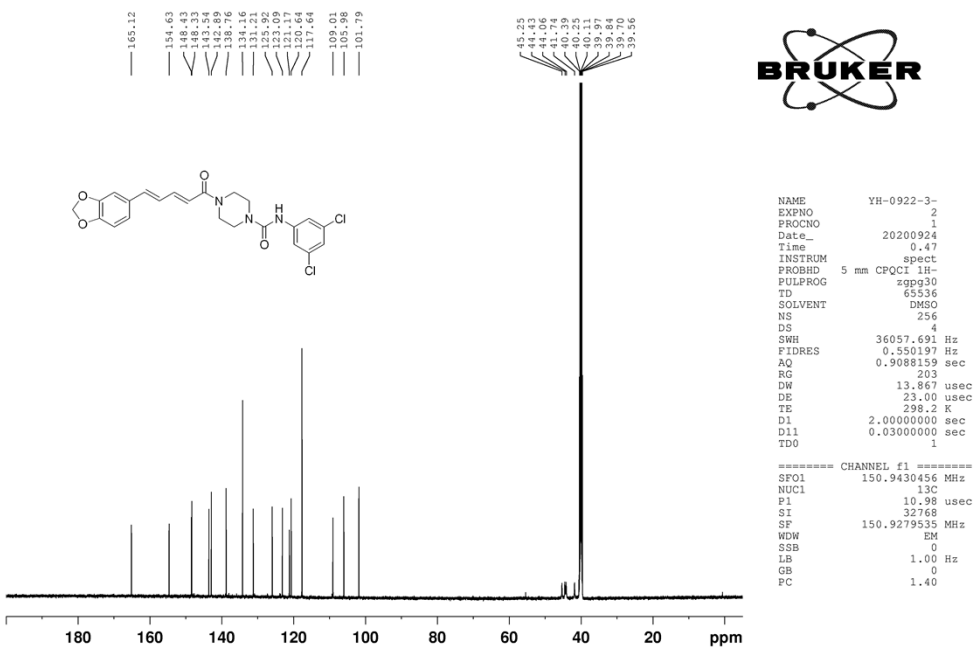

Fig. S39 ^{13}C-NMR spectrum of compound **11e**

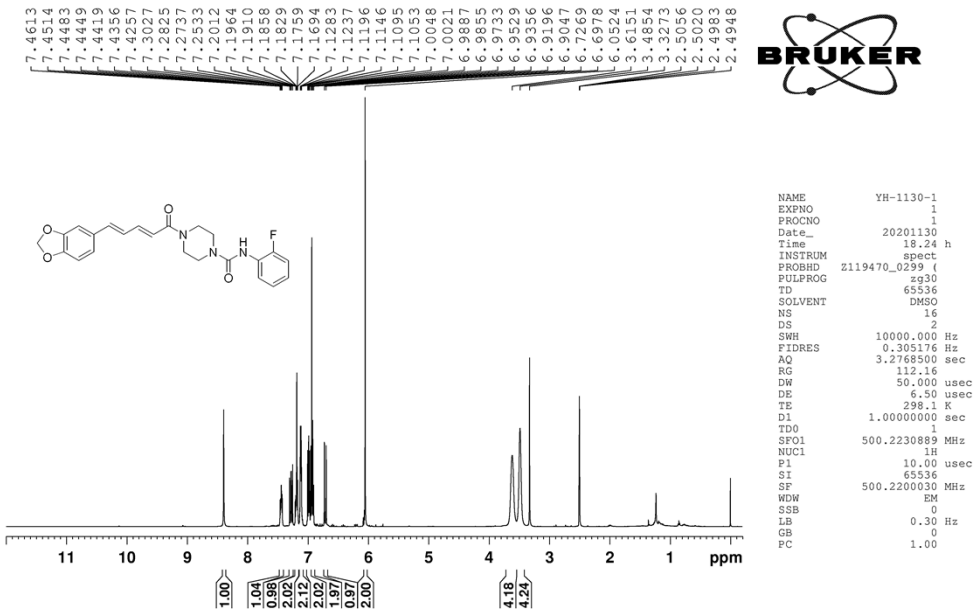

Fig. S40 ^{1}H-NMR spectrum of compound **11f**

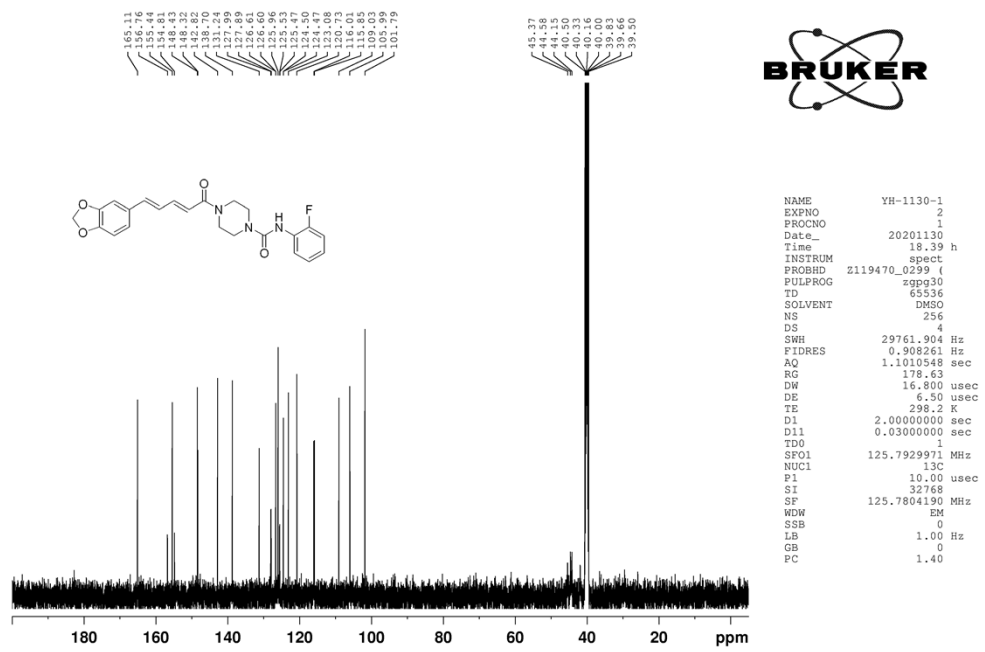

Fig. S41 ^{13}C-NMR spectrum of compound **11f**

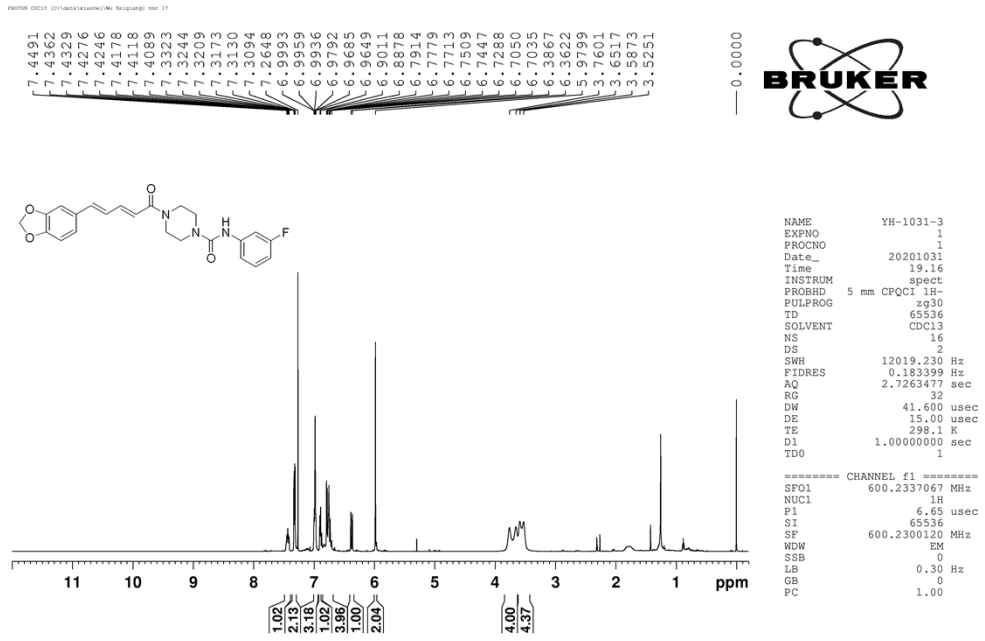

Fig. S42 ^{1}H-NMR spectrum of compound **11g**

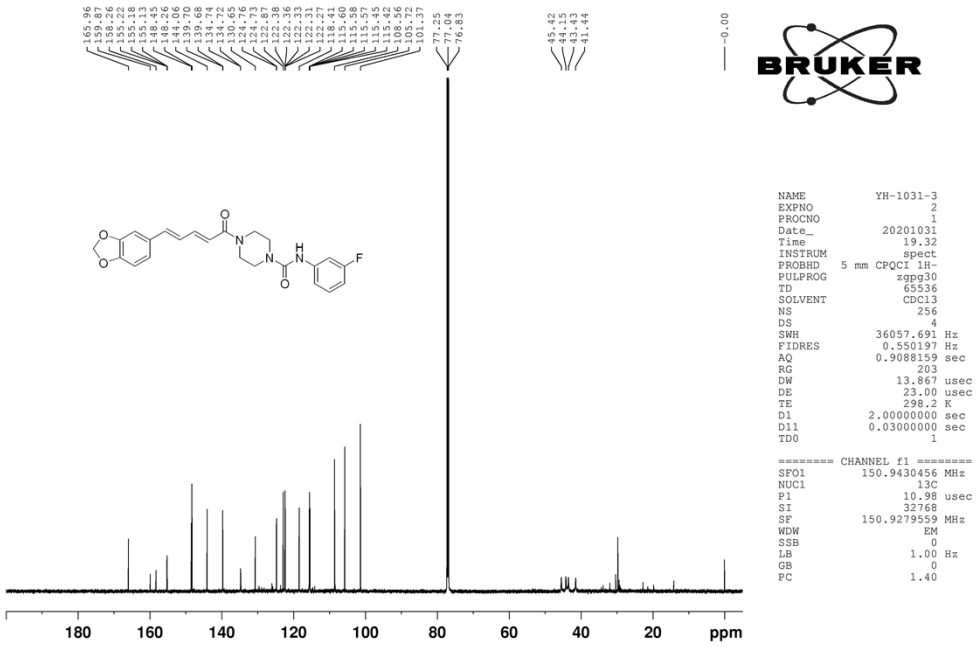

Fig. S43 ^{13}C-NMR spectrum of compound **11g**

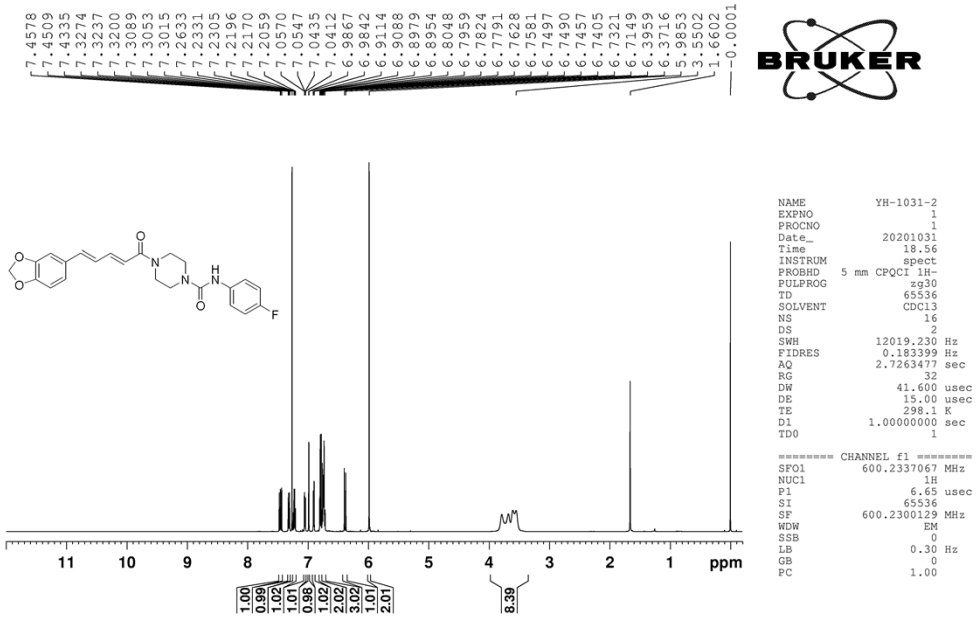

Fig. S44 ^{1}H-NMR spectrum of compound **11h**

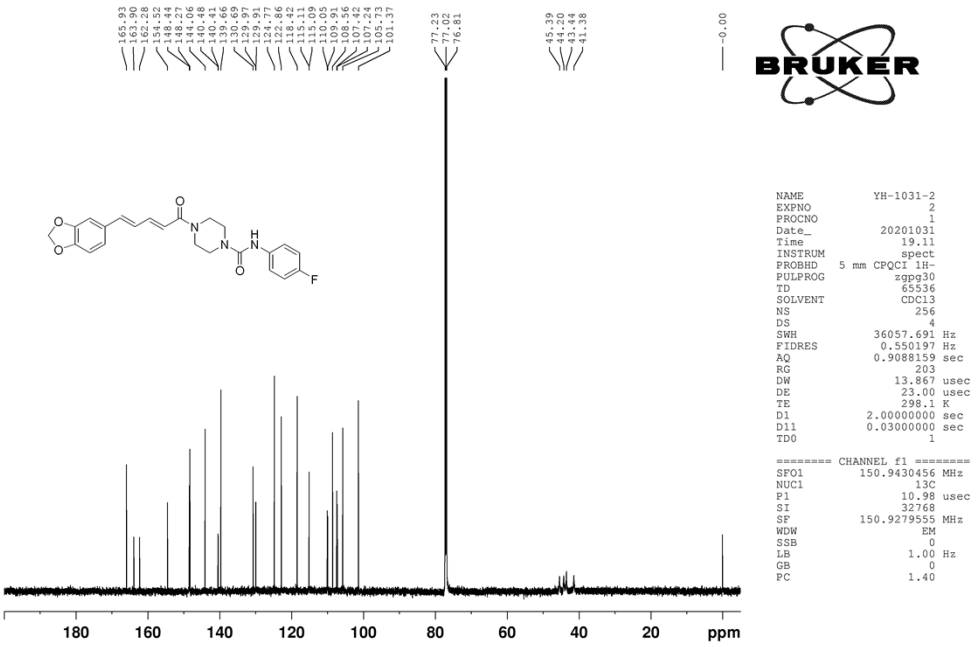

Fig. S45 ^{13}C-NMR spectrum of compound **11h**

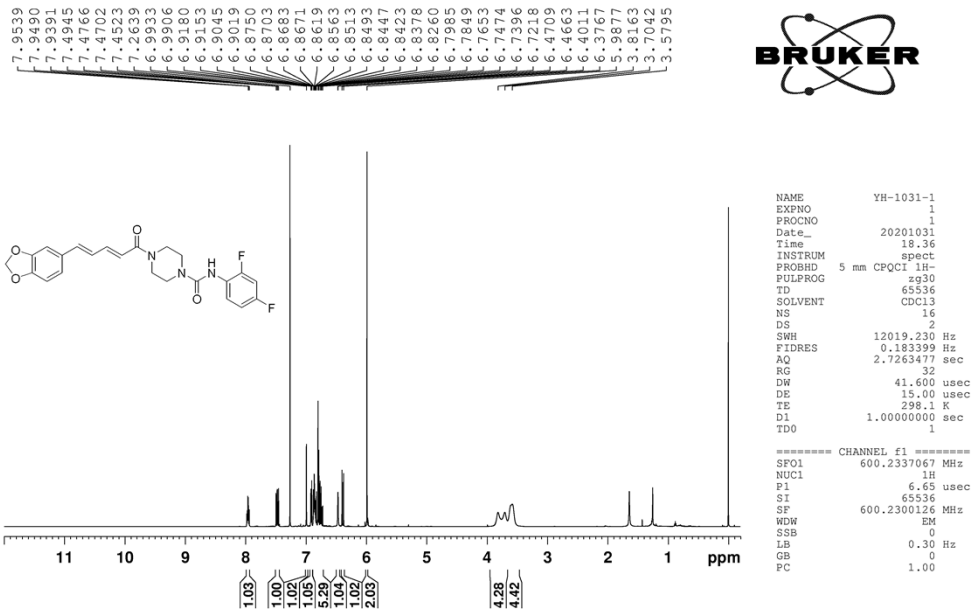

Fig. S46 ^{1}H-NMR spectrum of compound **11i**

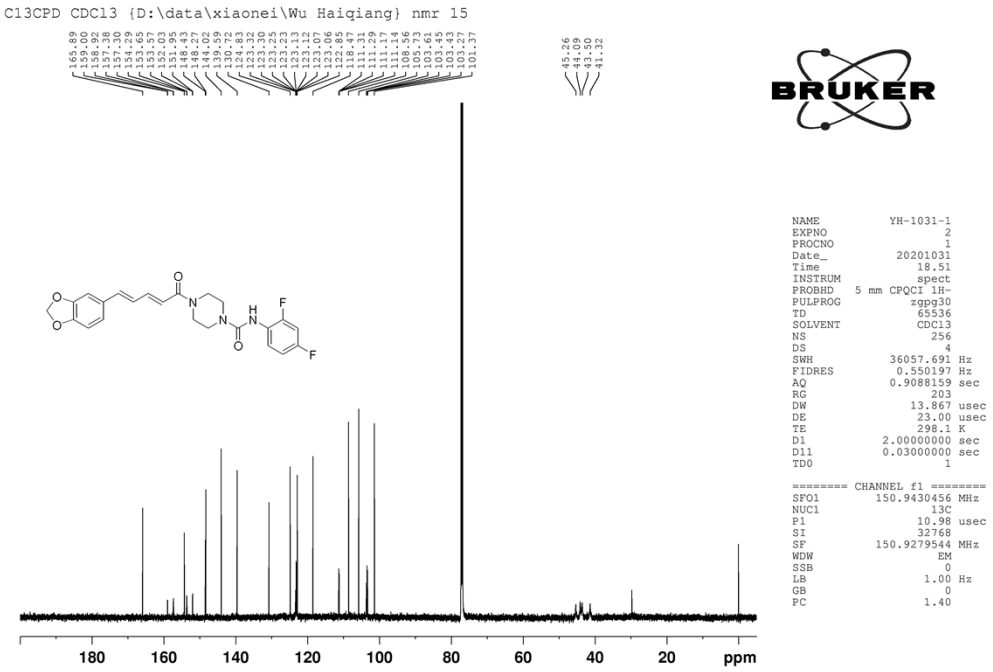

Fig. S47 ^{13}C-NMR spectrum of compound **11i**